NATIONAL ADVISORY COMMITTEE FOR AERONAUTICS

TECHNICAL NOTE 2292

EXPERIMENTAL INVESTIGATION OF THE EFFECTS OF SUPPORT INTERFERENCE ON THE DRAG OF BODIES OF REVOLUTION AT A MACH NUMBER OF 1.5

By Edward W. Perkins

Ames Aeronautical Laboratory
Moffett Field, Calif.

Washington
February 1951

NATIONAL ADVISORY COMMITTEE FOR AERONAUTICS

TECHNICAL NOTE 2292

EXPERIMENTAL INVESTIGATION OF THE EFFECTS OF SUPPORT INTERFERENCE ON THE DRAG OF BODIES OF REVOLUTION AT A MACH NUMBER OF 1.5

By Edward W. Perkins

SUMMARY

Tests were conducted to evaluate the effects of support interference on the drag characteristics of two bodies of revolution at zero angle of attack and at a Mach number of 1.5. The models, which varied only in their afterbody shape, were tested in the smooth condition and with roughness added to determine the support-interference effects for both laminar and turbulent flow in the boundary layer. Drag and base-pressure measurements were made for most tests over a range of Reynolds numbers, based on model length, of from 0.6 million to 5.0 millions to determine the effect of varying the length or diameter of the rear support. A side support in combination with a rear support was used to evaluate the magnitude of the interference. The schlieren method was used to determine the effect of the support on the flow over the afterbody of the models.

For the body of revolution with zero boattailing and either laminar or turbulent flow in the boundary layer, the fore drag was not affected by the rear support; however, the base drag and, therefore, the total drag depended on the support configuration used. The base drag was found to depend on the diameter of the rear support over the complete range of rear-support diameters used in the investigation, but was independent of changes in support length as long as the support length was at least 5.2 body diameters.

For the body of revolution with appreciable boattailing and laminar flow in the boundary layer, both the base drag and the fore drag were independent of changes in the length or diameter of the rear support as long as the length was equal to or greater than 1.7 body diameters and the diameter was equal to or less than 0.4 body diameter.

For the body of revolution with boattailing and turbulent flow in the boundary layer, the fore drag was not affected by the rear support. As before, the base drag was not affected by changes in length or diameter of the support as long as the length was equal to or greater than 1.7 body diameters and the diameter was equal to or less than 0.40 body diameter.

For a body of revolution without boattailing and with a laminar boundary layer, drag results which are essentially interference-free were obtained by the use of a suitable rear support, the dimensions of which are practical for wind-tunnel testing. For this same body with a turbulent boundary layer, sufficient data were not obtained on which to base a similar conclusion.

INTRODUCTION

Since the ultimate aim of wind-tunnel investigations is to aid the designer in predicting the aerodynamic characteristics of full-scale aircraft in free flight, it is essential that the interference effects encountered in wind-tunnel testing be understood and taken into account in the presentation and use of published data. A considerable amount of both theoretical and experimental work has been published concerning this problem for subsonic speeds, but as yet very little is available for supersonic speeds.

Preliminary tests conducted in preparation for the investigation reported in reference 1 showed that the relative size of the rear supports in common use had a large effect on the measured drag of bodies of revolution. In addition, these interference effects were found to depend on the afterbody shape of the model as well as the test Reynolds number. Therefore, since the investigation of reference 1 was concerned only with the effect of Reynolds number on the drag of bodies of revolution, it was first necessary to evaluate the interference effects of the rear supports on the drag characteristics of the models to be used in that program. The results of that preliminary series of tests are the basis for the statements concerning the support interference which appear in reference 1.

It was subsequently decided to conduct a more comprehensive study of the support-interference problem to check these preliminary results and to extend the scope of the investigation. The present report is based on the results of these latter tests combined with some of the results of the preliminary tests. The data presented herein were included in a classified document issued in 1948.

APPARATUS AND TEST METHODS

Wind Tunnel and Instrumentation

This investigation was conducted in the Ames 1- by 3-foot supersonic wind tunnel No. 1, a variable-pressure tunnel equipped during this investigation with a fixed nozzle designed to provide a test-section Mach number of 1.5. The drag force on each model was determined by means of an electrical strain-gage balance system. The pressure acting on the base of the model was measured by manometers which were connected to a pressure orifice in the base of the model. A schlieren apparatus was used to observe the flow field about the test models. A more detailed description of the wind tunnel, the balance system, and the additional instrumentation is presented in references 1 and 2.

Models and Supports

Photographs of the models used in this investigation are shown in figure 1, and all pertinent dimensions are given in figure 2. Since these models are the same models that were used in the investigation reported in reference 1, the numbering system used therein has been retained. Models 1 and 3 were used primarily for the determination of the effects of support interference on the drag of bodies with and without boat tailing. The forebodies of these models were formed of 10-caliber ogives followed by short cylindrical sections. The models differed only in the boat tailing of the afterbody. In addition to the two basic models, a substitute ogive having the same dimensions as the nose sections of these models was used to evaluate the increment of drag due to the addition of the roughness that was employed to promote boundary-layer transition.

Two different support systems were used separately and in combination. Cutaway drawings and photographs of a typical model installation on each support are shown in figures 3, 4, and 5. The rear support consisted of a sting of circular cross section that attached to the balance beam. Aerodynamic tare forces were avoided by enclosing the sting in a thin shroud which was attached to the balance cap. Two series of shrouds were employed such that the position of the model with respect to the balance cap, and the outside diameter of the shroud relative to the diameter of the model, were systematically varied. Force data, base-pressure data, and schlieren photographs were obtained when the model was supported from the rear.

The side support which consisted of a symmetrical, 6-percent-thick airfoil with straight-side segments and a 7° semiwedge angle at the leading and trailing edges, supported the model from the lower side. The models were attached to the side support so that the leading edge of the support coincided with the beginning of the cylindrical section of the afterbody, except for one series of tests (fig. 22(c)) in which the model was attached to the side support at approximately one body diameter ahead of the base of the model. Base-pressure data and schlieren photographs were obtained when the side support was used.

Test Methods

The test procedures employed in this investigation were essentially the same as those described in reference 1. In order to eliminate the effect of the axial pressure gradient in the test section as a variable, the models occupied the same streamwise postion whenever possible.

Models 1 and 3 were tested throughout the available Reynolds number range with a series of rear supports to determine the effect on the measured drag of, first, varying the support length with a constant diameter, and second, varying the support diameter while maintaining the length constant. Each of these tests were then repeated with the addition of roughness to fix transition. The models were then tested in the smooth condition with the side support alone and finally with the side support and a dummy rear support.

The method used to fix transition was to cement a 1/8-inch-wide band of particles of table salt around the body at the beginning of the cylindrical section. This is the same artifice used in reference 1 and, as before, was successful in causing complete transition of the boundary layer at all but the very low Reynolds numbers.

To determine the magnitude of the additional wave drag attributable to the salt band, the substitute ogive with no afterbody attached and full-diameter shrouding was tested, first, in the smooth condition, and then with roughness added. The results of these tests, which were repeated several times, are presented in figure 6. It is evident from this plot that, even though in each instance an attempt was made to add equal amounts of salt to the ogive, the additional wave drag which can be attributed to the salt band may vary considerably between two apparently identical tests. This observation is also

borne out by consideration of the magnitude of the experimental scatter in the fore-drag data in several of the figures (e.g., figs. 15 and 20) which include tests of models 1 and 3 made with the salt band added to promote transition.

An average value of the wave drag due to the salt particles, as represented by the difference between the curve for the smooth ogive and the dotted curve, has been subtracted from all subsequent data presented. It is gratifying to note that this average value of the wave drag differs only slightly from that previously determined in reference 1, even though those results were based on only one test of the model with roughness added. The knowledge gained from these present tests, as to possible variation of the incremental wave drag due to the salt band caused by inadvertent differences in the character of the salt bands, is equally applicable to the results presented in reference 1 for the models tested with roughness added. In comparing the data in this report with those presented in reference 1 for the models tested with roughness added, these possible variations should be kept in mind.

ANALYSIS OF DATA

Reduction of the Data

The results of the force tests have been reduced to the usual coefficient form, and are referred to frontal area of the body and the free-stream dynamic pressure as determined from conditions just ahead of the nose of the model. The base-drag coefficients are calculated from the equation

$$C_{D_b} = -\frac{p_b - p_o}{q_o}\left(\frac{A_b}{A}\right)$$

where

C_{D_b} base-drag coefficient

p_o free-stream static pressure

p_b pressure acting on the base

q_o free-stream dynamic pressure

A_b area of the base

A frontal area of the model

The fore drag is defined as the sum of all the drag forces that act on the surface ahead of the base and hence is obtained experimentally as the difference between the total drag and the base drag. The Reynolds number is based on body length.

The procedure followed in applying corrections to the measured coefficients to account for the effect of the axial variation of test-section static pressure is the same as reported in Appendix A of reference 1. For example, these corrections to the measured coefficients of model 1 in most instances were +0.012 in fore-drag coefficient and −0.026 in base-drag coefficient; the corresponding percentages of the uncorrected fore-drag and base-drag coefficients are 12 and 15, respectively.

Two dimensionless parameters are used to describe the support dimensions. These are l/D and d/D, in which l is the "effective length" of the support which has been taken as the distance from the base of the model to the beginning of the balance cap, D is the diameter of the cylindrical portion of the models, and d is the outside diameter of the shroud which encloses the sting.

Precision

Some possible uncertainties exist in each of the individual measurements which go into the determination of the drag coefficients. An estimate of the total uncertainty of the drag coefficients has been determined in this report by geometric summation of the individual uncertainties rather than by the algebraic summation that was employed in reference 1. The details of the evaluation of these possible uncertainties in the individual measurements are considered extensively in Appendix B of reference 1 and, therefore, only the results which are applicable to this investigation are presented here. The following table, which applies to the tests of the models in the smooth condition only, indicates the estimated uncertainty which might appear in each of the drag coefficients at two values of the Reynolds number:

	Model 1		Model 3	
	Re=0.8 × 10^6	Re=4.3 × 10^6	Re=0.8 × 10^6	Re=4.3 × 10^6
Base-drag coefficient	±4%	±2½%	±6½%	±4½%
Fore-drag coefficient	±4%	±3½%	±3½%	±2%
Total-drag coefficient	±3%	±1½%	±3%	±1½%

For the models tested with roughness added, an additional uncertainty exists due to the indeterminate wave drag of the salt band as previously noted. This uncertainty, which applies to both the fore-drag and the total-drag coefficients, may be as much as ±0.01. It is believed that even though this uncertainty does exist it does not invalidate any of the qualitative conclusions which have been drawn from the data.

Schlieren Photographs

Schlieren photographs are used to indicate the effect of the variations in support configuration upon the flow characteristics about the models. A typical schlieren picture, in which some of the features of flow are designated, is presented in figure 7. In addition, a schlieren picture with the wind off is included which shows the striae in the glass windows that form the tunnel side walls at the test section. These striae appear in the background of all the schlieren photographs. The photographs were taken with the knife edge vertical, that is, perpendicular to the stream direction, thereby accentuating density gradients in a streamwise direction. The orientation of the knife edge with respect to the stream was such that increasing positive density gradients in the downstream direction appear as white areas (except in fig. 7(a) in which the shock waves appear as dark areas due to different orientation of the knife edge).

DISCUSSION

Flow Characteristics

Before presenting the quantitative data on the effects of the rear support on the measured-drag characteristics of the bodies of revolution, it is advantageous to first indicate some of the qualitative effects on the flow characteristics so that the reasons for these quantitative effects may be more apparent.

It was shown in reference 1 that the condition of the boundary layer (laminar or turbulent), which could be easily determined from schlieren pictures and force tests, had a marked effect on the flow pattern in the vicinity of the base of a body of revolution immersed in a supersonic stream. The location and degree of separation of a laminar boundary layer, which normally occurred on the boat-tailed portion of the body, varied noticeably with the Reynolds number of flow. In each case, as the Reynolds number was increased, the degree of flow separation decreased, the convergence of the wake increased, and the trailing shock wave moved forward. Changing the flow in the boundary layer from laminar to fully developed turbulent flow greatly increased the resistance of the boundary layer to flow separation. Changes in flow separation which were brought about by changes in either Reynolds number or the condition of the boundary layer altered the effective shape of the body, the shock-wave configuration in the vicinity of the base, and the measured drag.

These changes in convergence of the wake, shock-wave configuration, and measured drag, associated in reference 1 with changes in Reynolds number or the condition of the boundary layer, can also be caused by changes in the rear-support configuration.

Convergence of the wake.- In reference 1 it was pointed out that the convergence of the wake behind the models tested with a laminar boundary layer increased with increasing Reynolds number. In the present series of tests it was found that, for model 1, this same phenomenon (change in convergence of the wake) accompanied changes in either the length or diameter of the rear support even though the Reynolds number was held constant. In addition, it was found that these changes in convergence of the wake occurred for the model tested with either a laminar or a turbulent boundary layer.

The schlieren pictures of figure 8, which are typical of these effects, show that increases in length of the rear support from 0.7 body diameter to 2.4 body diameters are accompanied by large increases

in the convergence of the wake. Further increases in support length do not appear to affect appreciably the wake convergence. Comparison of the pictures which show this effect for the model tested with a laminar boundary layer, (fig. 8(a)), with those for the model tested with a turbulent boundary layer (fig. 8(b)) shows that not only does the convergence of the wake increase with increases in length of the support in both cases, but also that the range of support lengths over which this effect is apparent is approximately the same.

Although it is not immediately apparent from the schlieren pictures of figure 8, a careful study of the original negatives of these pictures shows that increasing the diameter of the rear support for model 1 with either a laminar or a turbulent boundary layer results in increases in the convergence of the wake, even though the Reynolds number is held constant. This is a somewhat surprising result since it might be expected that increasing the diameter of the rear support would cause the wake to converge less rapidly or, in fact, possibly to diverge.

Since models 1 and 3 differ only in their boat tailing, it might be expected that changing the length or diameter of the rear support would, for model 3, cause changes in the convergence of the wake similar to those observed for model 1. Yet, in contrast to those results, the schlieren pictures of figure 9(a), which are of model 3 with a laminar boundary layer, show that the convergence of the wake is not affected by changes in the length or diameter of the rear support until the support length is reduced to less than 1.7 body diameters, or the support diameter increased to greater than 0.40 body diameter. Beyond these values the convergence of the wake decreases. In terms of the diameter of the base of the model rather than the diameter of the cylindrical section, these ratios are 2.9 base diameters and 0.70 base diameter, respectively.

For model 3 with a turbulent boundary layer, no conclusions as to the convergence of the wake can be drawn from the schlieren pictures of figure 9(b), since the wake is obscured by the shock wave which is attached to the base of the model.

Shock-wave configuration.- In reference 1 it was shown that changes in flow separation, due to changes in the condition of the boundary layer and in the Reynolds number of the flow, brought about changes in the shock-wave configuration at the base of the body. In general, as long as the boundary layer was laminar, the flow separation decreased and the trailing shock moved forward with increases in Reynolds number, but no major change in the shock-wave configuration took place. In the present investigation it was found that changes

in the position and character of the trailing shock wave can be induced by changes in the rear-support dimensions even at a constant Reynolds number.

Since the trailing shock wave originates from the wake behind a model, it might be expected that any influence that alters the characteristics of the wake will, in addition, have some effect on the trailing shock wave.

The schlieren pictures of figure 8 show that, as the length of the rear support is increased from 0.7 body diameter to 1.7 body diameters for model 1 with either a laminar or a turbulent boundary layer, the convergence of the wake increases but the trailing shock wave moves downstream. This is opposed to the observation made in reference 1 with regards to the effect of changes in Reynolds number on the position of the trailing shock wave. As shown in reference 1, increases in the Reynolds number for a model tested with a laminar boundary layer also resulted in increased convergence of the wake; however, in that instance, the trailing shock moved upstream rather than downstream. The reason for this apparent paradox is that, for support lengths less than 1.7 body diameters, the shock wave behind the base of the body is not truly a trailing shock wave originating from the wake but rather a combination of the shock wave originating from the beginning of the balance cap and the trailing shock wave. Thus, as the support length is decreased, the balance cap is moved closer to the base and the shock wave from the beginning of the balance cap predominates. Therefore, the combined shock waves move closer to the model even though the convergence of the wake decreases.

As shown in figure 8, increases in diameter of the rear support for model 1, with either a laminar or turbulent boundary layer and at a constant Reynolds number, are accompanied by increases in convergence of the wake and thus an upstream shift of the trailing shock wave. In the limiting case, where the diameter of the support is equal to the diameter of the base of the model, the trailing shock wave attaches itself to the base of the model. This shock wave is probably due to the gap between the base of the model and the shroud.

For model 3 at a constant Reynolds number and with a laminar boundary layer, the schlieren pictures of figure 9 show that changes in length of the support do not affect the convergence of the wake until the length of the support is less than 1.7 body diameters. Consequently, the location of the trailing shock wave is not altered until the configuration is analagous to that previously noted for model 1 in which the support is so short that the shock wave from the beginning of the balance cap interferes with the trailing shock wave.

As the diameter of the rear support is increased for model 3, with a laminar boundary layer and at a constant Reynolds number (fig. 9), the trailing shock wave moves upstream even though there is no apparent change in the convergence of the wake until the diameter of the support is almost equal to the diameter of the base of the model. The reason for this upstream movement of the trailing shock wave in the absence of increasing convergence of the wake is purely one of geometry. The flow over the afterbody of the model and the point of laminar separation are not influenced by the changes in the rear support; therefore, as the diameter of the support is increased, the angle of incidence of the separated boundary layer is such that the intersection of the converging boundary layer and the support occurs progressively further upstream. As pointed out in the previous section, a change in the convergence of the wake is noted only in the instance where the largest diameter support was used.

The only apparent change in the shock-wave configuration at the base of model 3 with a turbulent boundary layer, that occurs at constant Reynolds number with changes in the rear-support dimensions, is a forward movement of the base shock wave. This forward movement occurs only when the model is mounted on the minimum length or maximum diameter rear support. In these instances the so-called base shock wave actually occurs upstream of the base of the model.

Analysis of the Drag Data

The changes in flow characteristics in the vicinity of the base of the model which accompany changes in the rear-support geometry, form a basis for understanding the effects of the rear supports on the measured drag of the models. As has been pointed out in the previous section, changes in flow configurations similar to those associated with either changes in the Reynolds number of flow or the condition of the boundary layer can be attributed to changes in the rear-support dimensions. As will be pointed out in the subsequent discussion, varying the support dimensions in such a manner as to cause changes in the flow pattern similar to those which accompany changes in the Reynolds number or condition of the boundary layer results in changes in the measured drag characteristics which are comparable.

In the subsequent discussion it is convenient to consider the effect of changes in rear-support configuration on the measured drag of each model tested, first, with a laminar boundary layer,

and then with a turbulent boundary layer. For each model with a laminar boundary layer the effects of changes in length or diameter of the support are considered separately; whereas for each model tested with a turbulent boundary layer these effects are considered together since the primary interest lies in whether or not the previously observed interference effects are altered by the presence of a turbulent boundary layer on the model.

Model 1 with laminar flow: effect of support length.- The measured drag characteristics of model 1 as affected by changes in length of a constant-diameter rear support ($d/D = 0.3$) are shown in figure 10. The parameter used in this plot is the ratio of the effective support length to the maximum diameter of the model. From these results it is evident that the fore drag of this model is not affected by changes in support length; whereas the base drag and therefore the total drag vary with the effective length of the support. This is to be expected since, as the schlieren pictures indicate, changes in the flow pattern about the body which accompany changes in the effective length of the support are confined to those changes which occur in the convergence of the wake and the position of the trailing shock wave. Therefore, only those forces which depend on the flow aft of the base should be affected.

In reference 1 it was observed that the increase in convergence of the wake, which accompanied increases in the Reynolds number of flow, resulted in lower base pressures and thus higher base drags. Similarly (as shown by fig. 11, which is a cross plot of the data of fig. 10), increasing the effective support length up to 2.4 body diameters, which has been shown to cause increased convergence of the wake, resulted in higher base drags. At any Reynolds number the base-drag coefficient is more than doubled by increasing the effective support length from 0.7 body diameter to 2.4 body diameters. Although it was impossible to discern from the schlieren pictures any further change in convergence of the wake accompanying increases in the length of the support from 4.1 to 5.2 body diameters, the base-drag coefficient decreased approximately 10 percent. Further increases from 5.2 to 7.2 body diameters had no apparent effect on either the convergence of the wake or the base drag.

No attempt has been made to define the curves of figure 11 in the region $l/D = 2.4$ to $l/D = 4.1$, since no tests were conducted in this range and the schlieren pictures of figure 8(a) show that the shock-wave configuration changes from one in which the trailing shock wave and the shock wave from the beginning of the balance cap coincide to one in which the two shock waves occur separately. Little

if any change in the convergence of the wake accompanies this change in shock-wave configuration.

Model 1 with laminar flow: effect of support diameter.- The variation of the total-drag, fore-drag, and base-drag coefficients as a function of the Reynolds number for model 1, with a series of rear supports of various diameters, is shown in figure 12. For convenience in the model setup, the lengths of this series of supports were allowed to vary over a small range for which $4.1 \leqq l/D \leqq 5.4$. Although this variation of support length has some effect on the quantitative drag values, it does not alter any of the general conclusions of the investigation. Here again it is noted that, as in the case of changes in support length, the fore drag is not affected by changes in the support diameter. Thus the interference effects of the rear support on the drag of this model tested with a laminar boundary layer are confined to their influence on the pressure acting over the base.

The variation of the base-drag coefficient with changes in the support diameter is shown in figure 13, which is a cross plot of the data presented in figure 12, and thus includes the effects of the small changes in support length as previously noted. This variation of base-drag coefficient is easily explained on the basis of the observed changes in convergence of the wake. The schlieren pictures show that, as the diameter of the support is increased, the convergence of the wake behind the body increases and the trailing shock wave moves forward. As previously indicated, these changes in flow are accompanied by a decrease in base pressure and a consequent increase in base drag. As the diameter of the rear support is increased beyond the point where the base drag is a maximum, the schlieren pictures show that the wake no longer converges sharply but appears to flow over the shroud with only slight convergence to the point where the trailing shock wave occurs. Thus with increasing support diameter the base-drag coefficient increases to a maximum, the magnitude of which depends on the Reynolds number. Further increases in support diameter result in a sharp decrease in the base-drag coefficient.

Model 1 with turbulent flow: effect of support length and diameter.- The effect of changes in length of a constant-diameter rear support on the drag characteristics of model 1 with roughness added to cause a turbulent boundary layer are presented in figure 14. The effects of changing the diameter of the support are shown in figure 15. The individual lengths of this series of supports were varied from 4.0 to 5.4 body diameters.

For model 1, the effects on the flow pattern of changing the length or diameter of the rear support have been shown to be the same for either a laminar or turbulent boundary layer on the body. Therefore, it might be expected that the existence of a turbulent rather than a laminar boundary layer would not materially alter the nature of the interference effects on the drag characteristics of the model. The variation of the base-drag coefficient with the support length at various Reynolds numbers for model 1 with a turbulent boundary layer is shown in figure 16. A comparison of this figure with figure 11, the equivalent curve for model 1 with a laminar boundary layer, shows that the qualitative effects of the rear support on the measured drag does not depend on the condition of the boundary layer. This observation is further substantiated by comparison of figures 17 and 13 which are equivalent curves showing the effect of the rear-support diameter on the measured drag for model 1 with a turbulent and laminar boundary layer, respectively.

As before, increases in support length are accompanied by increases in base drag to the same limits of l/D, beyond which further increases in support length are ineffective. Similarly, the base-drag coefficient first increases with increasing support diameter to a maximum, the value of which depends on the test Reynolds number, then decreases sharply with further increases in support diameter. For a support diameter equal to the diameter of the model base, the compression through the shock wave at the base of the model (fig. 8(b)) is sufficient to raise the base pressure above free stream and thus produce a thrust on the base of the model. This increase in base pressure to a value above free stream probably would not occur if the gap between the base of the model and the shroud were eliminated, since, as was previously pointed out, the occurrence of the shock wave is dependent on the existence of this gap.

Model 3 with laminar flow: effect of support length.- The measured-drag characteristics of model 3 as affected by changes in length of a constant-diameter rear support ($d/D = 0.3$) are shown in figure 18. From these results it is evident that the support length may be reduced to at least 1.7 body diameters without effecting any change in the drag characteristics. This critical support length corresponds to that previously noted with regards to changes in wake convergence attributable to changes in support length.

As contrasted to the results for model 1, the fore drag as well as the base drag of model 3 is affected by the support interference. The explanation of this behavior is found in a consideration of the flow over the boat-tailed portion of the model. As presented in reference 1 and shown in the schlieren pictures of figure 9(a), the boundary layer separates from the body in flowing over the boat tail

Therefore, the pressure disturbances in the wake caused by the presence of the rear support are propagated upstream through the "dead-water" region accompanying the separated flow. Thus, for this boat-tailed model, any object in the wake affects both the base pressure and the pressures acting over the boat tail and hence both the base drag and fore drag.

As the Reynolds number of flow is increased, the decrement in fore drag due to the presence of the rear support decreases; whereas the interference effects on the base pressure increase. This effect on the fore drag is reasonable since, as the Reynolds number is increased, the degree of laminar separation for this type body decreases, as previously shown in reference 1. Therefore the boat-tail area, over which the pressure in the dead-water region acts, decreases and consequently the interference effects on the fore drag are less. These results indicate that, if flow separation does not occur, the fore drag of a body will not be appreciably affected by the presence of the rear support. This condition is realized for model 1, and for model 3 tested with a turbulent boundary layer, and in each case, it was found that the fore drag was independent of the rear-support configuration.

The reason for the decrease in base-drag coefficient with increasing Reynolds number with the support length equal to 0.7 body diameter is evident from schlieren pictures which show that the trailing shock wave moves upstream and at a Reynolds number of about 2.5 millions attaches itself to the base of the model. The compression through this shock wave increases the pressure acting over the base of the model and therefore decreases the base-drag coefficient.

Model 3 with laminar flow: effect of support diameter.- The variation of the total drag, fore drag, and base drag, as a function of Reynolds number for model 3 with a series of rear supports of various diameters, is shown in figure 19. The lengths of the rear supports were held constant at 4.1 body diameters. Increasing the diameter of the rear support had no effect on the drag characteristics until the ratio of support diameter to body diameter exceeded a critical value of 0.40. In terms of the ratio of support diameter to base diameter, this critical value is approximately 0.7. The schlieren pictures of figure 9(a) indicate that up to this critical diameter ratio the increase in shroud diameter is accompanied by a forward movement of the trailing shock wave, but the convergence of the wake remains essentially unchanged.

The use of a large support $d/D = 0.55$ resulted in a marked decrease in both the base-drag and the fore-drag coefficients. As

before, the decrement in fore drag due to the support interference decreased with increasing Reynolds number due to the smaller region of separated flow, but in this instance the decrement in base-drag coefficient remained essentially constant and no base shock wave was apparent.

Model 3 with turbulent flow: effect of support length and diameter.- Figures 20 and 21 show the effects of the geometry of the rear supports on the measured drag characteristics of model 3 with roughness added to cause a turbulent boundary layer. These curves are dotted in the region where the force measurements and the schlieren pictures indicate that the desired transition was not achieved. Except for the fore drag, the presence of the turbulent boundary layer does not materially alter the nature of the effects of the rear supports on the measured drag characteristics. As previously found for the model tested in the smooth condition, the length of the rear support must be reduced to less than 1.7 body diameters or the support diameter increased to greater than 0.40 body diameter before any effects of support interference are evident. In this instance, as contrasted to the results obtained for the model tested in the smooth condition, the fore drag is not affected by changes in the support configuration, since as shown in the schlieren pictures of figure 9(b) the addition of roughness has caused a turbulent boundary layer which does not separate in flowing over the boat tail. Therefore the pressure disturbances in the wake caused by the presence of the rear support have no appreciable effect on the pressures acting over the boat-tail portion of the body. The differences in the fore-drag curves of figures 20 and 21 are attributed to the differerences in the character of the salt bands as previously discussed.

It is interesting to note from figure 9(b) that the base shock wave originates immediately at the base of the model in all cases except where the model is mounted on the minimum length or the maximum diameter supports. In each of these instances the base shock wave originates some distance ahead of the base. This forward movement of the shock wave is probably caused by the increased back pressure in the wake due to the size and proximity of the rear support, and is accompanied by an increase in base pressure and consequent decrease in base-drag coefficient as evident from figures 20 and 21.

Determination of the Interference-Free Base-Drag Characteristics

The experimental determination of the interference-free base-drag characteristics for the models tested in the smooth condition

is based upon the assumption that at any test Reynolds number the effect of the rear support on the base pressure is equal to the difference in the base pressure measured with the model supported by the side support alone, and the base pressure for the model supported by the side support and the rear support in combination. This method of evaluation assumes that the mutual interference between the rear support and side support is negligibly small. If this were strictly true, the effect on the base pressure of varying either the support diameter or support length should be independent of the presence or absence of the side support.

Model 1.- A comparison of the change in base pressure resulting from an increase in rear-support diameter of from 0.30 to 0.60, with and without the side support in place, indicates that for this model the assumption is good above Reynolds numbers of 2 millions; whereas at lower Reynolds numbers mutual interference, which may be as large as 10 percent of the measured data, is indicated. The results which follow are based upon the assumption of negligible mutual interference, and thus may be somewhat in error at the lower Reynolds numbers.

The results of the tests to determine the interference-free base drag characteristics of model 1 tested with a smooth surface are presented in figure 22. The interference-free results for each combination of supports are deduced by determining, at any Reynolds number, the algebraic difference between the curve for the model mounted on the side support plus the dummy rear support and the curve for the model mounted on the side support alone. This difference thus represents the effect of the dummy rear support and, when added to the curve for the model mounted on the rear support alone, results in interference-free base-drag data. By repeating this process of addition and subtraction for the complete range of Reynolds numbers, a curve representing the interference-free base-drag characteristics can be obtained.

The curves in figure 22(d), each deduced from different combinations of side support and rear support, are compared and a mean curve drawn which thus represents the best estimate of the interference-free base-drag characteristics of model 1 tested in the smooth condition.

A comparison of this interference-free base-drag data with the data presented in figure 13 on the effect of varying the diameter of the rear support indicates that at any Reynolds number the base-drag coefficients obtained with the smallest diameter support used were always less than the interference-free values. This is surprising since the linear nature of these curves with decreasing support

diameter leads one to believe that extrapolation of the curves to zero support diameter ratio would predict the interference-free base drag values. No physical explanation for this behavior is yet apparent, although it is possible that this case is analogous to the subsonic results reported by Zobel in reference 3 wherein a large increase in pressure over the rear portion of a model with a resulting decrease in drag was caused by the presence of an object in the wake.

The determination of interference-free drag characteristics in this manner requires two support systems which can be used independently or in combination, and three separate tests of the model covering the same Reynolds number range. Since it would be advantageous to be able to evaluate the aerodynamic-drag characteristics with only one test, the deduced interference-free results were compared with those previously obtained with a rear support alone. It was found that for model 1 the base-drag data which compared most favorably was obtained with the rear-support configuration ($d/D = 0.35$, $l/D = 4.1$). As a matter of fact, the base drag coefficients agree exactly at a Reynolds number of 4 millions and differ by only 2 percent at a Reynolds number of 2 millions, the difference varying almost linearly between these limits. Therefore, it is possible to evaluate the aerodynamic drag over the Reynolds number range of from 2 to 4 millions and within the experimental accuracy of this investigation for model 1 with a rear support of the dimensions indicated. It should be noted that the error incurred in the base-drag coefficient by the use of this optimum rear support is only 1-1/4 percent of the total drag at the higher Reynolds numbers, which is well within the limits of the experimental accuracy of this investigation.

If reference 4 it was concluded that the conditions at the base of a model in a supersonic wind tunnel are unaffected by the presence of the windshield as long as a convergent wake exists, and also that the base pressure obtained with a convergent wake correspond to that of free flight.

The present investigation, however, has shown that at a Mach number of 1.5 the presence of the windshield or balance cap does affect the conditions at the base of the model even though the wake is convergent. In addition, it was shown that the base pressure depends on the length and diameter of the rear support even though the wake converges behind the body for all the combinations of support dimensions used. The model used in the tests of reference 4 was a conical model with a 10° semivertical angle and a cylindrical afterbody 0.312 inch in diameter. The test Mach number was 3.2, the minimum length and the

diameter of the support were 1.62 inches and 0.125 inch, respectively.

It is interesting to note that the minimum support length of 5.2 body diameters for convergence of the wake determined in reference 4 agrees exactly with the minimum length corresponding to zero interference due to the balance cap determined in the present investigation. This suggests that for models with a flat base and zero boat tailing the effect of the length of support is zero for support lengths greater than 5.2 body diameters and for Mach numbers greater than 1.5.

The support diameter equal to 0.4 body diameter used in the tests of reference 4 corresponds very closely to the support diameter for zero interference effects, as determined in the present series of tests wherein the optimum diameter for interference-free data varies between 0.3 and 0.4 body diameter depending on the test Reynolds number.

Model 3.- An attempt was made to determine the interference-free base-drag characteristics of model 3 based on the same assumptions previously indicated for model 1, but it was found that considerable mutual interference was encountered over the entire Reynolds number range of the tests. Thus it appears that at present the best estimate of the interference-free base-drag characteristics are those obtained for this model supported from the rear by a support for which $l/D > 1.7$ and $d/D < 0.4$.

It should be pointed out that for this model, for which the base drag is such a small part of the total drag, relatively large errors in the base drag result in only small errors in the total drag. If, for instance, we assume that the base-drag coefficient may be in error by as much as 25 percent, which is very unlikely, the resulting error in the total-drag coefficient will be only ± 5 percent.

CONCLUSIONS

The conclusions which follow apply for a Mach number of 1.5 and Reynolds numbers based on model length from 1 million to approximately 4.5 millions for bodies of revolution similar to the ones tested.

1. The magnitude of the effects of a rear support on the drag characteristics of a body of revolution depends on the afterbody shape, the type of boundary-layer flow, and the Reynolds number.

2. For a body of revolution with zero boat tailing with either laminar or turbulent flow in the boundary layer.

(a) The rear support affects the drag of the body through its immediate influence on the base pressure.

(b) The fore drag is not affected by the presence of a rear support.

3. For a body of revolution with appreciable boat tailing and laminar flow in the boundary layer, the rear support affects the drag of the model through its immediate effect on the pressures acting on the base of the model and in the region of separated flow over the boat-tailed portion of the afterbody.

4. For a body of revolution with appreciable boat tailing and turbulent flow in the boundary layer, the fore drag is not affected by the presence of a rear support.

5. For a body of revolution with zero boat tailing and with laminar flow in the boundary layer, drag results which are essentially interference free can be obtained in the higher Reynolds number range by the use of a suitable rear support, the dimensions of which are practical for wind-tunnel testing.

6. For a body of revolution with appreciable boat tailing and with laminar flow in the boundary layer, no conclusions as to interference-free base-drag data can be drawn from the available data, since considerable mutual interference between support systems was encountered in testing this configuration.

Ames Aeronautical Laboratory,
National Advisory Committee for Aeronautics,
Moffett Field, Calif., Jan. 28, 1948.

REFERENCES

1. Chapman, Dean R., and Perkins, Edward W.: Experimental Investigation of the Effects of Viscosity on the Drag of Bodies of Revolution at a Mach number of 1.5. NACA RM A7A31a, 1947.

2. Van Dyke, Milton D.: Aerodynamic Characteristics Including Scale Effect of Several Wings and Bodies Alone and in Combination at a Mach Number of 1.53. NACA RM A6K22, 1946.

3. Zobel: Advances in Optical Methods of Determining Air Flow. (Translation) Halstead Exploiting Centre BIOS/Gp.2/HEC No. 20 of forschungsbericht Nr. 1934.

4. Puckett, Allen E.: Final Report on the Model Supersonic Wind-Tunnel Project. National Defense Research Committee Armor and Ordnance Report No. A-269 (O.S.R.D. No. 3569) Division 2.

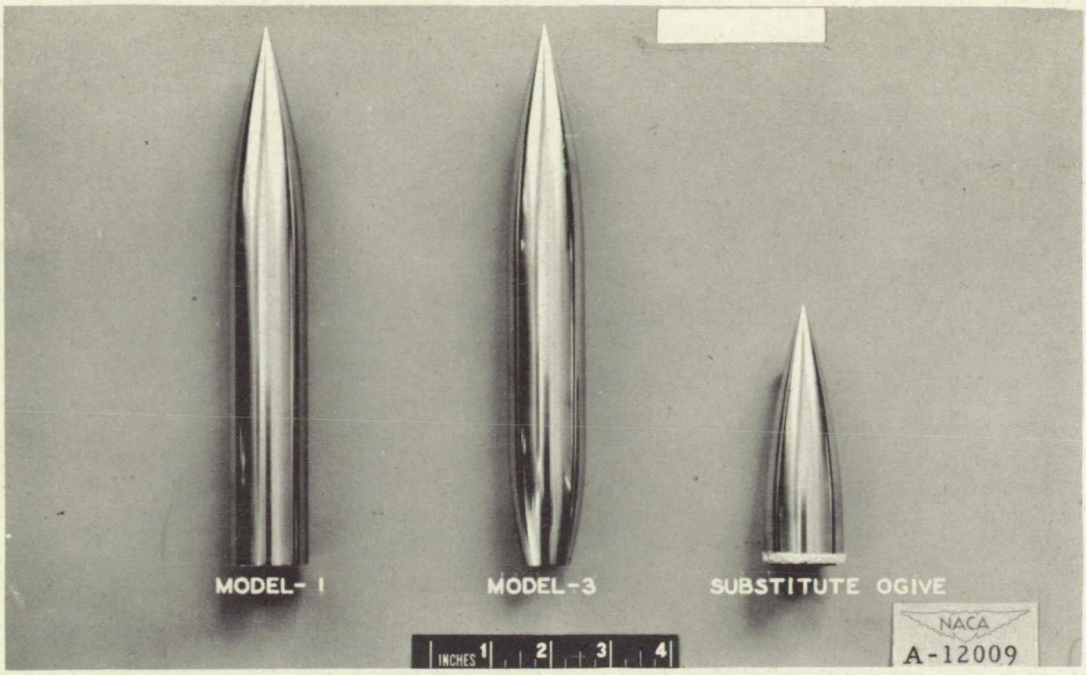

Figure 1.- Models used for the support interference investigation.

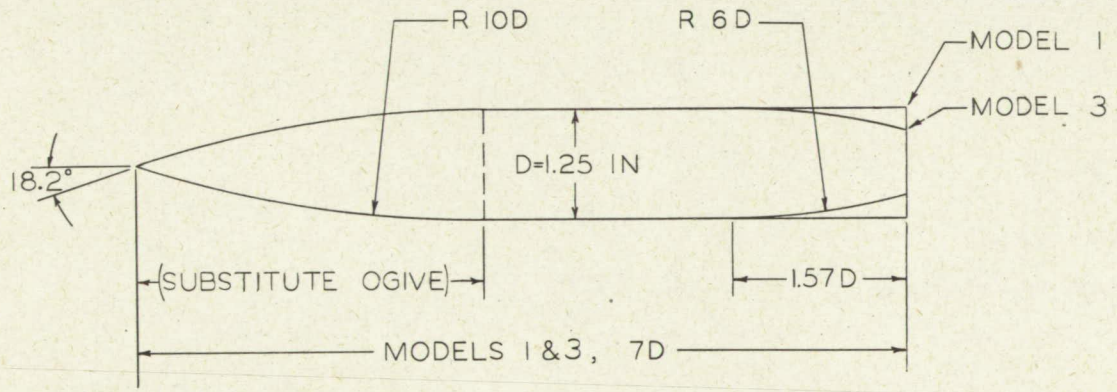

FIGURE 2.-MODEL DIMENSIONS

NACA
A-12010

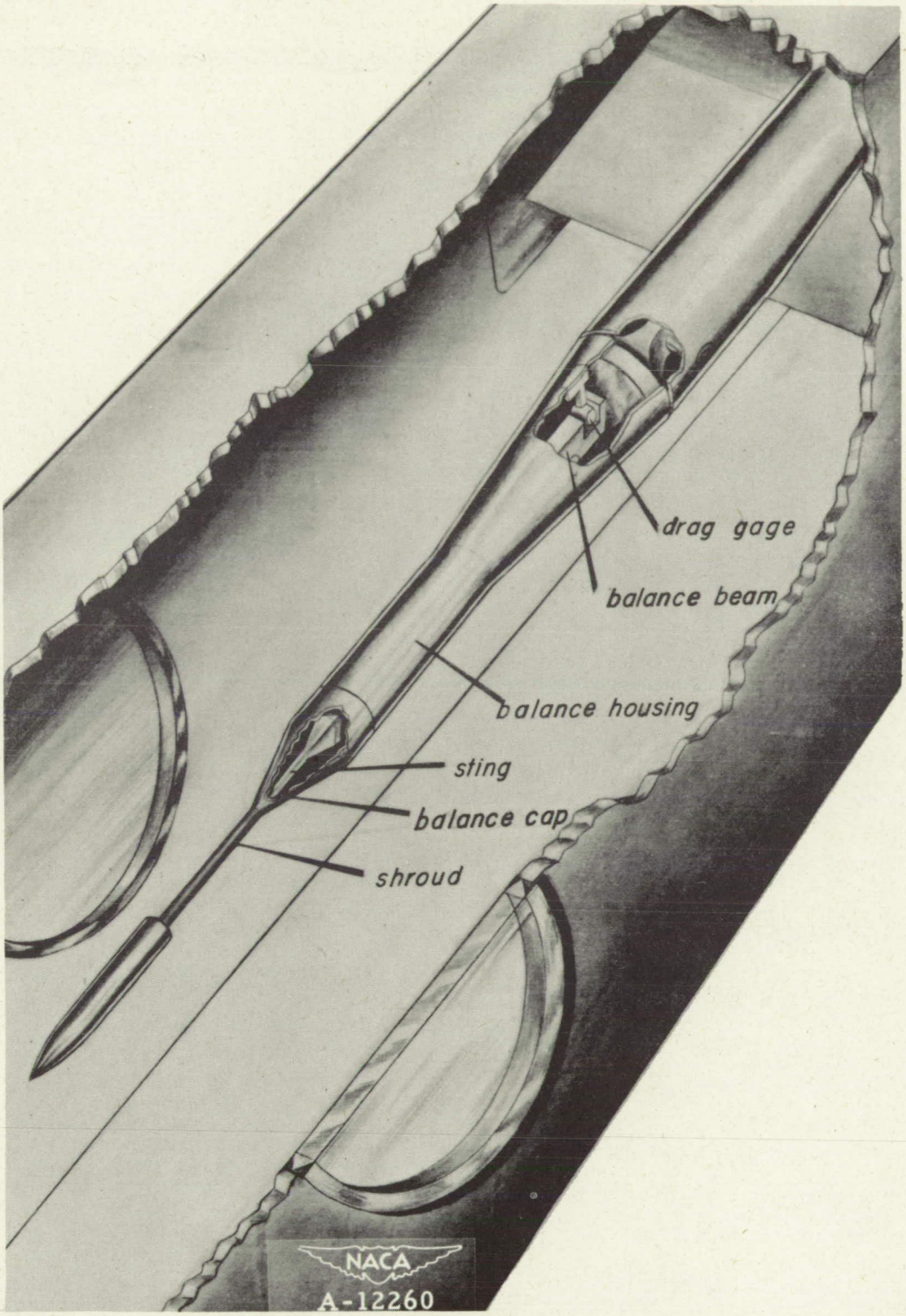

Figure 3.– Cutaway drawing of model 1 mounted on the rear support.

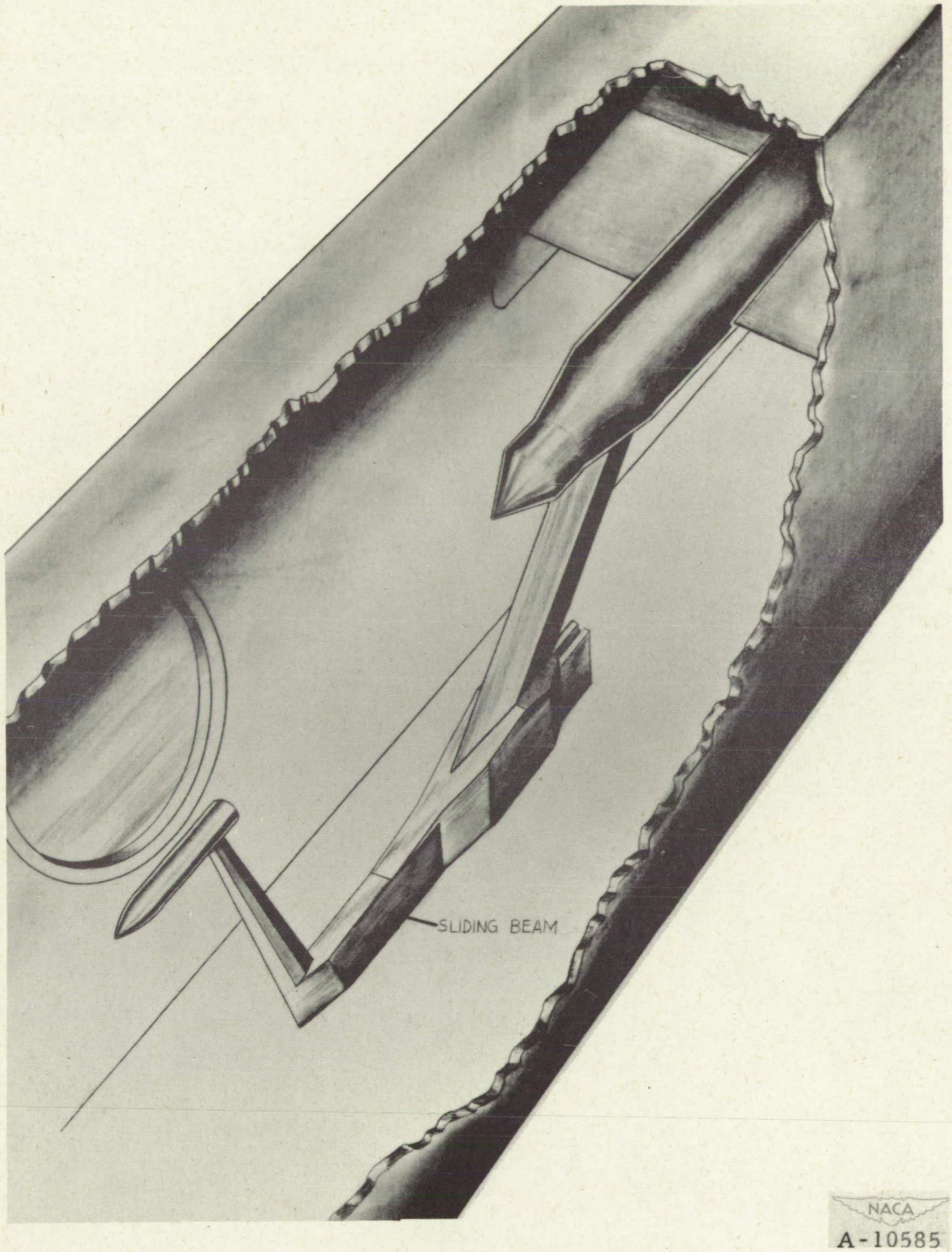

Figure 4.– Cutaway drawing of model 1 mounted on the side support.

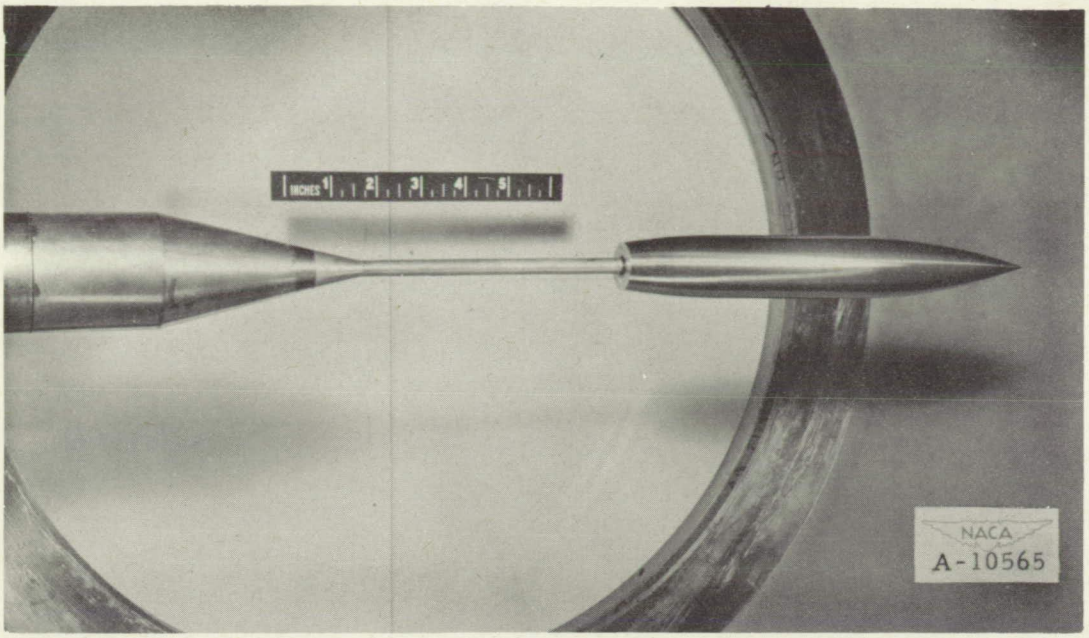

(a) Rear support.

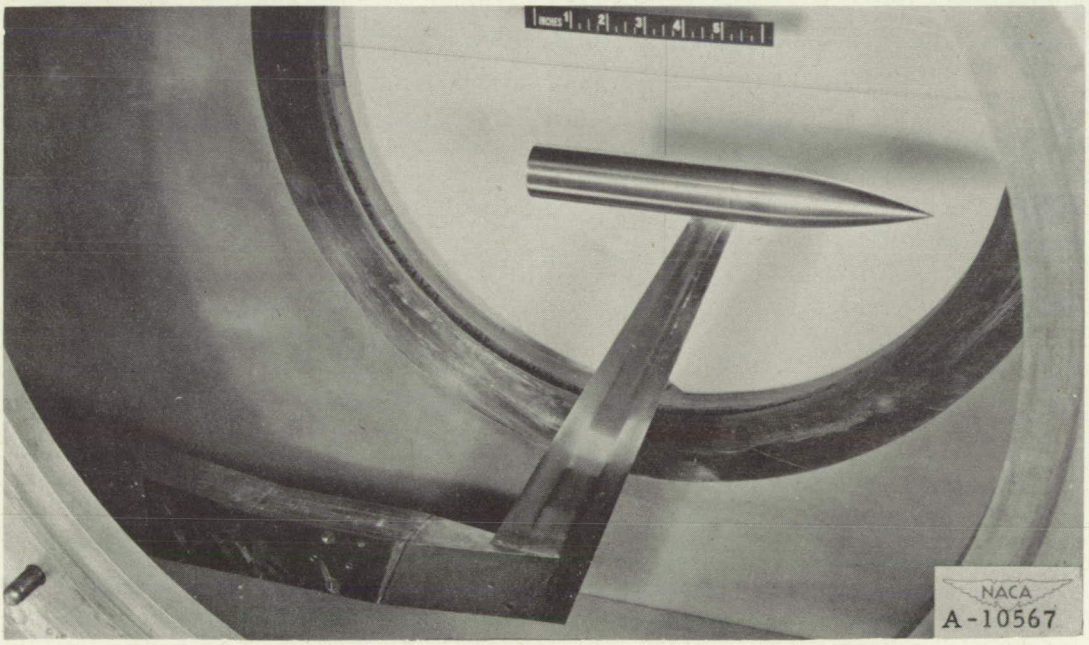

(b) Side support.

Figure 5.- Typical model installations.

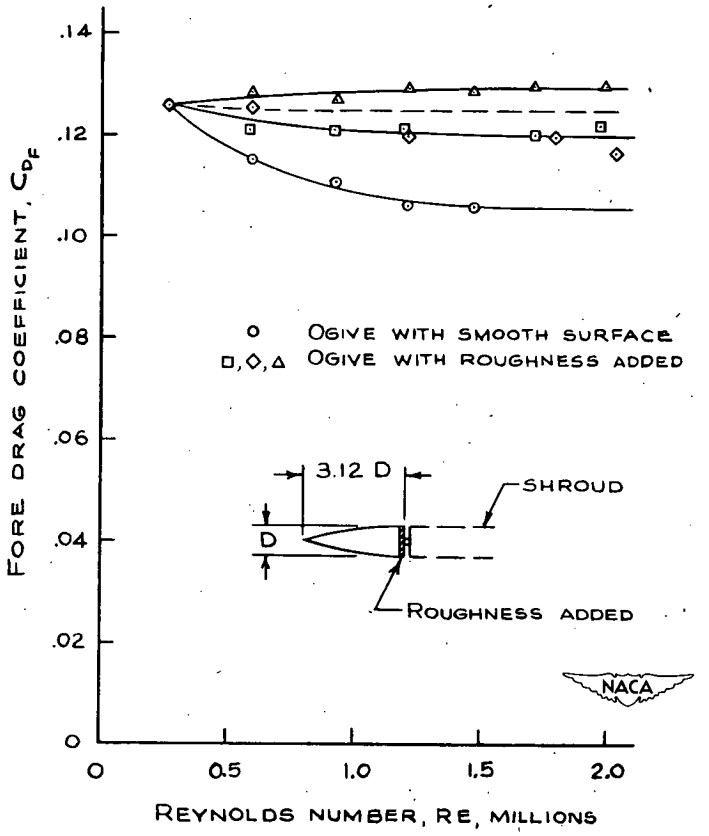

FIGURE 6.- FORE DRAG CHARACTERISTICS OF THE SUBSTITUTE OGIVE WITH AND WITHOUT ROUGHNESS ADDED.

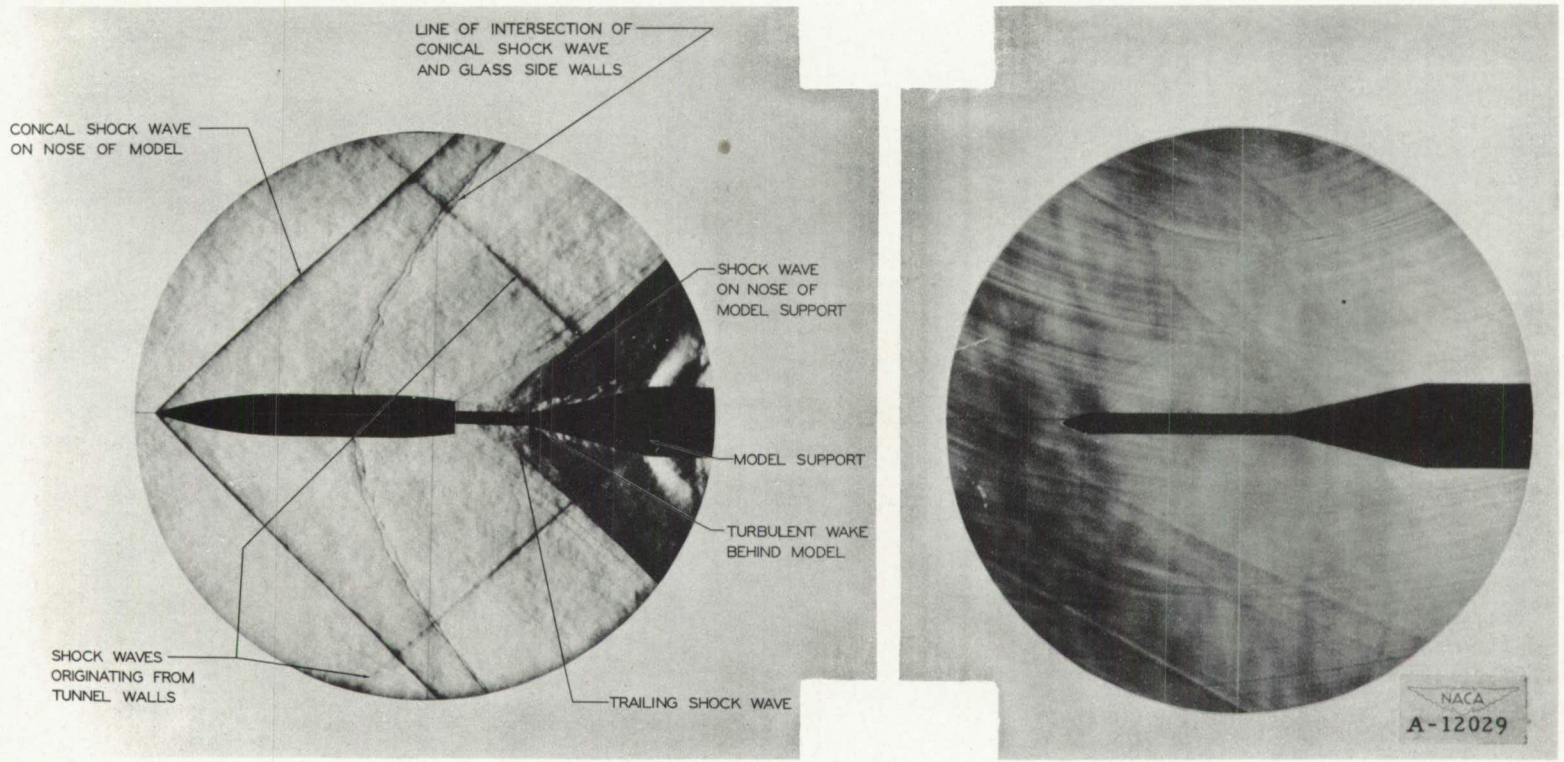

(a) Wind on.

(b) Wind off.

Figure 7.- Typical schlieren pictures.

Page intentionally left blank

Page intentionally left blank

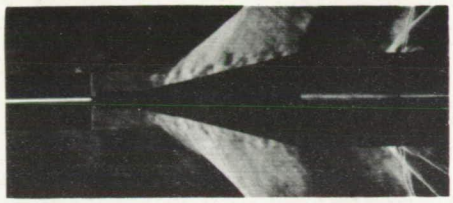

$l/D = 0.7$ $d/D = 0.3$

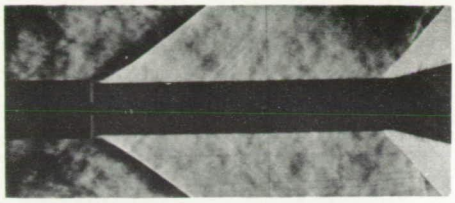

$d/D = 0.90$ $l/D = 5.2$

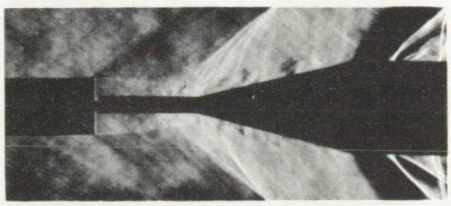

$l/D = 1.7$ $d/D = 0.3$

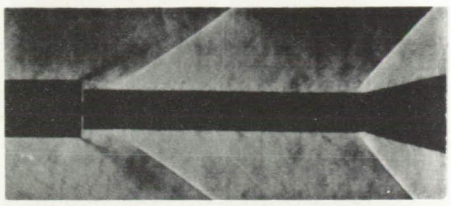

$d/D = 0.70$ $l/D = 4.8$

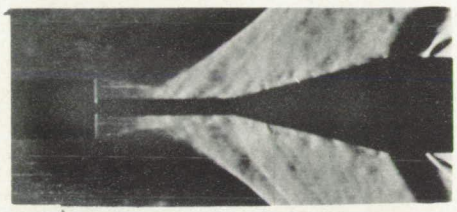

$l/D = 2.4$ $d/D = 0.3$

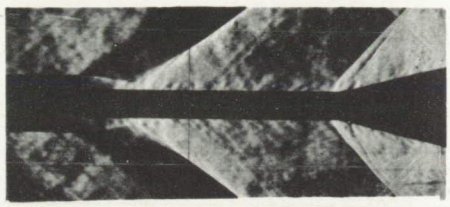

$d/D = 0.50$ $l/D = 4.4$

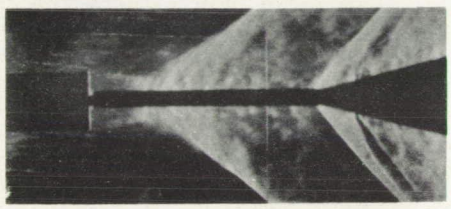

$l/D = 4.1$ $d/D = 0.3$

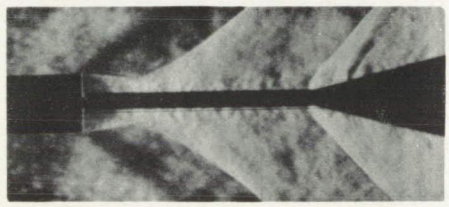

$d/D = 0.30$ $l/D = 4.1$

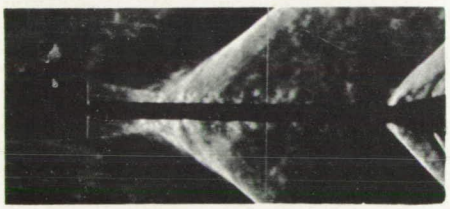

$l/D = 5.2$ $d/D = 0.3$

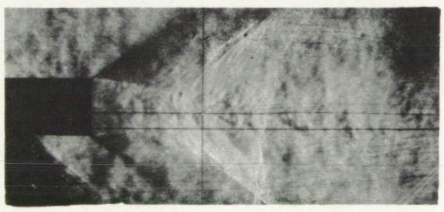

Side support

A-12492

(a) Laminar boundary layer.

Figure 8.– Schlieren pictures showing the changes in flow in the vicinity of the base of model 1 caused by altering the rear-support dimensions. Reynolds number = 3.8×10^6.

Page intentionally left blank

Page intentionally left blank

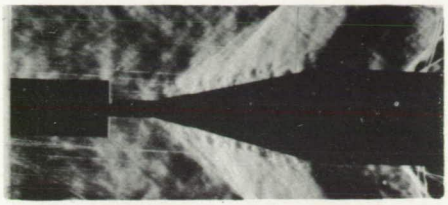

$l/D = 0.7$ $d/D = 0.3$

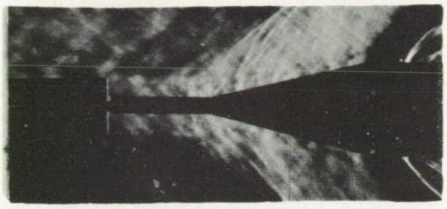

$l/D = 1.7$ $d/D = 0.3$

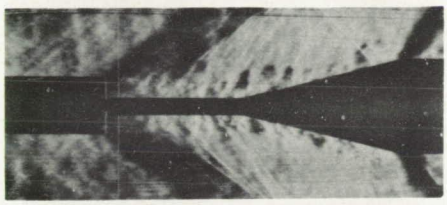

$l/D = 2.4$ $d/D = 0.3$

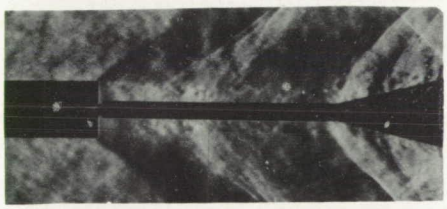

$l/D = 4.3$ $d/D = 0.3$

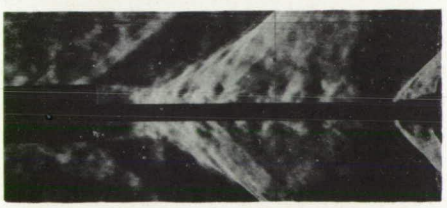

$l/D = 5.2$ $d/D = 0.3$

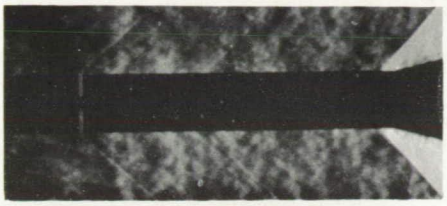

$d/D = 1.0$ $l/D = 5.6$

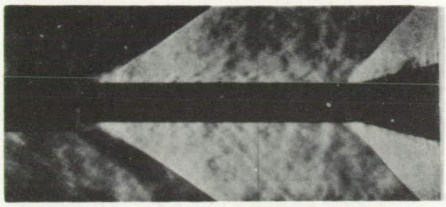

$d/D = 0.7$ $l/D = 5.0$

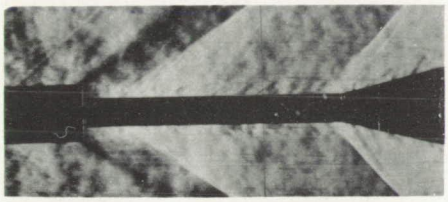

$d/D = 0.5$ $l/D = 4.6$

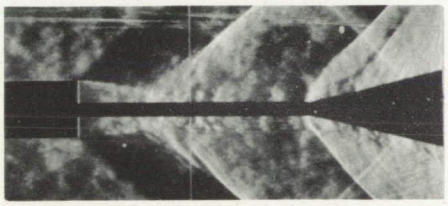

$d/D = 0.25$ $l/D = 4.1$

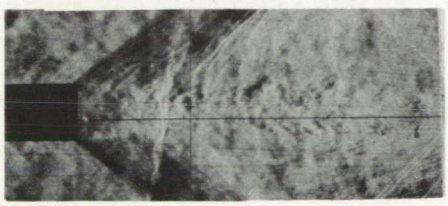

Side support

NACA

A-12493

(b) Turbulent boundary layer.

Figure 8.– Concluded.

Page intentionally left blank

Page intentionally left blank

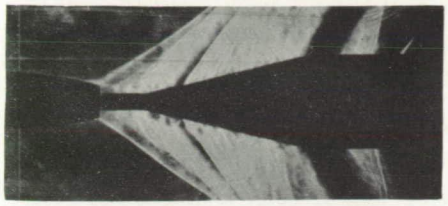

$l/D = 0.7$ $d/D = 0.3$

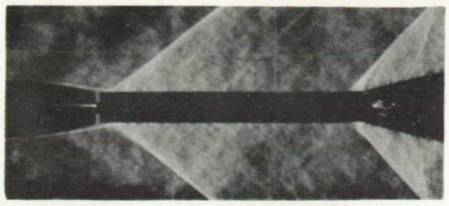

$d/D = 0.55$ $l/D = 4.8$

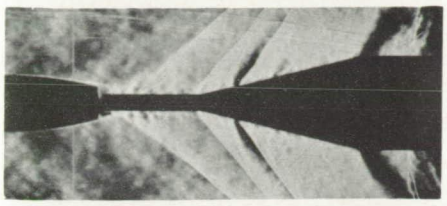

$l/D = 1.7$ $d/D = 0.3$

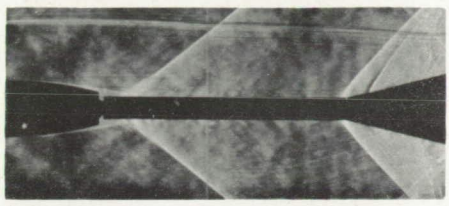

$d/D = 0.40$ $l/D = 4.7$

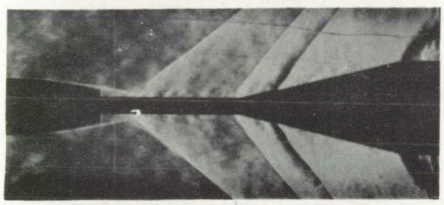

$l/D = 2.4$ $d/D = 0.3$

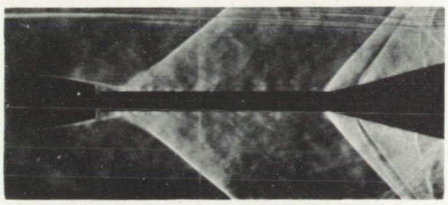

$d/D = 0.35$ $l/D = 4.0$

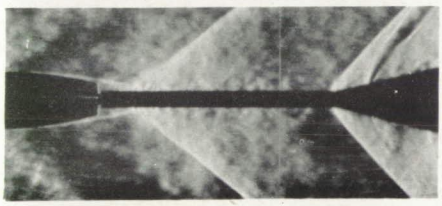

$l/D = 4.1$ $d/D = 0.3$

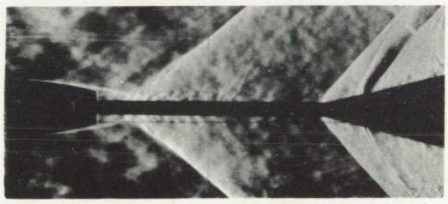

$d/D = 0.25$ $l/D = 4.0$

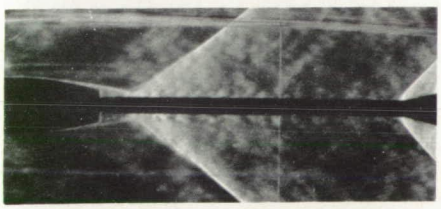

$l/D = 5.2$ $d/D = 0.3$

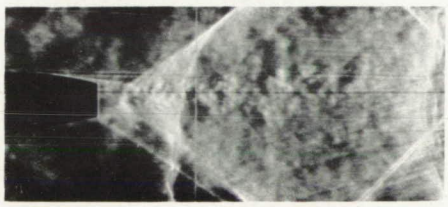

Side support

NACA

A-12494

(a) Laminar boundary layer.

Figure 9.– Schlieren pictures showing the changes in flow in the vicinity of the base of model 3 caused by altering the rear-support dimensions. Reynolds number = 3.8×10^6.

Page intentionally left blank

Page intentionally left blank

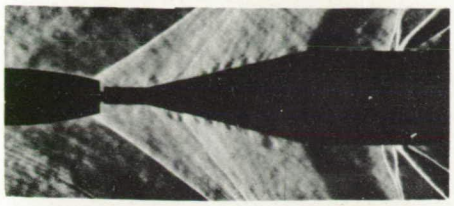

$l/D = 0.7$ $d/D = 0.3$

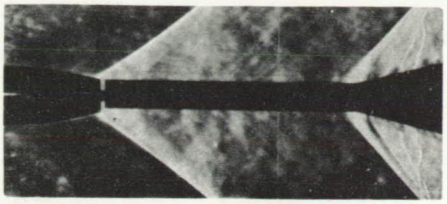

$d/D = 0.50$ $l/D = 4.4$

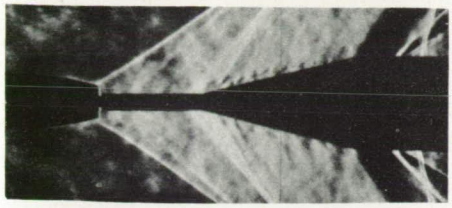

$l/D = 1.7$ $d/D = 0.3$

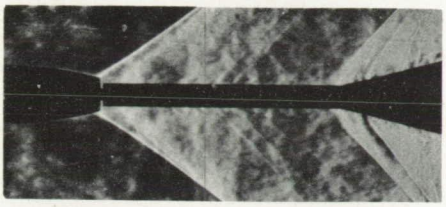

$d/D = 0.40$ $l/D = 4.2$

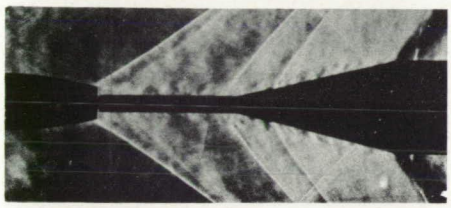

$l/D = 2.4$ $d/D = 0.3$

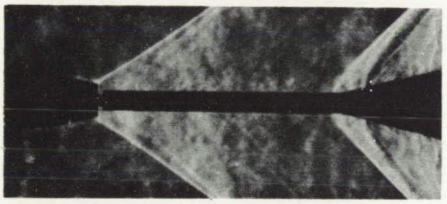

$d/D = 0.35$ $l/D = 4.0$

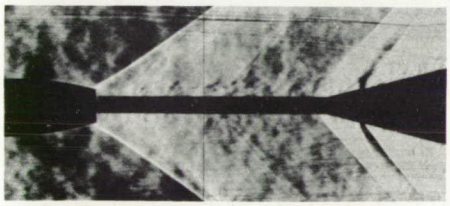

$l/D = 4.1$ $d/D = 0.3$

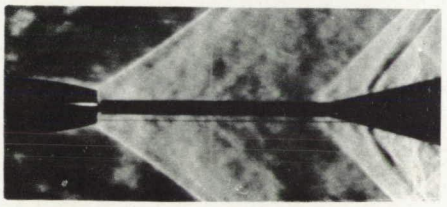

$d/D = 0.25$ $l/D = 4.0$

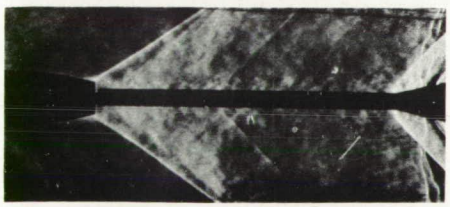

$l/D = 5.2$ $d/D = 0.3$

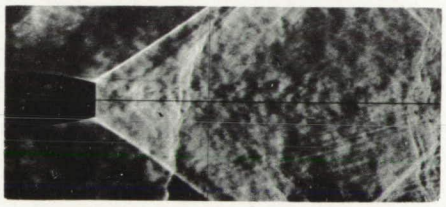

Side support

NACA

A-12495

(b) Turbulent boundary layer.

Figure 9.– Concluded.

Page intentionally left blank

Page intentionally left blank

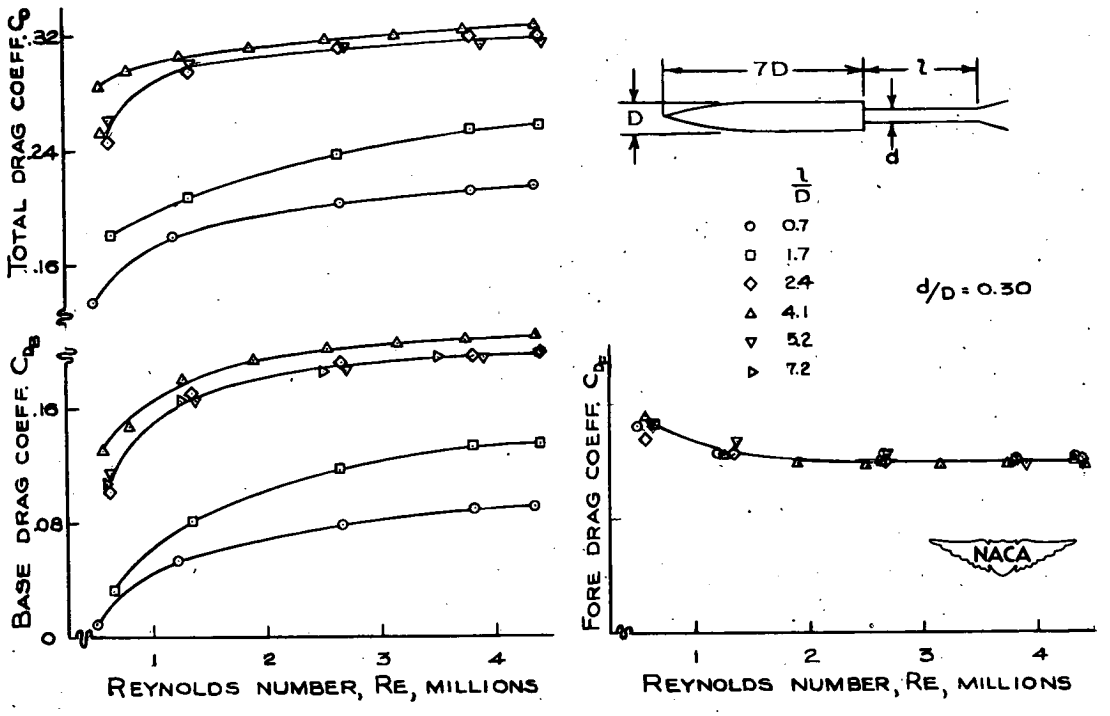

FIGURE 10.- VARIATION WITH REYNOLDS NUMBER OF THE DRAG CHARACTERISTICS OF MODEL 1 WITH SEVERAL REAR-SUPPORT LENGTHS.

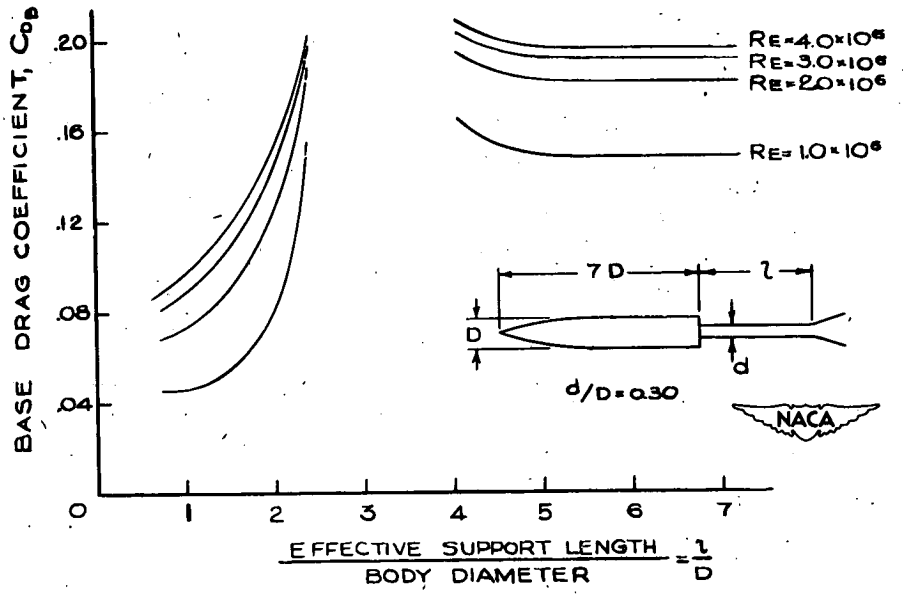

FIGURE 11.- VARIATION OF THE BASE DRAG COEFFICIENT WITH SUPPORT LENGTH FOR MODEL 1.

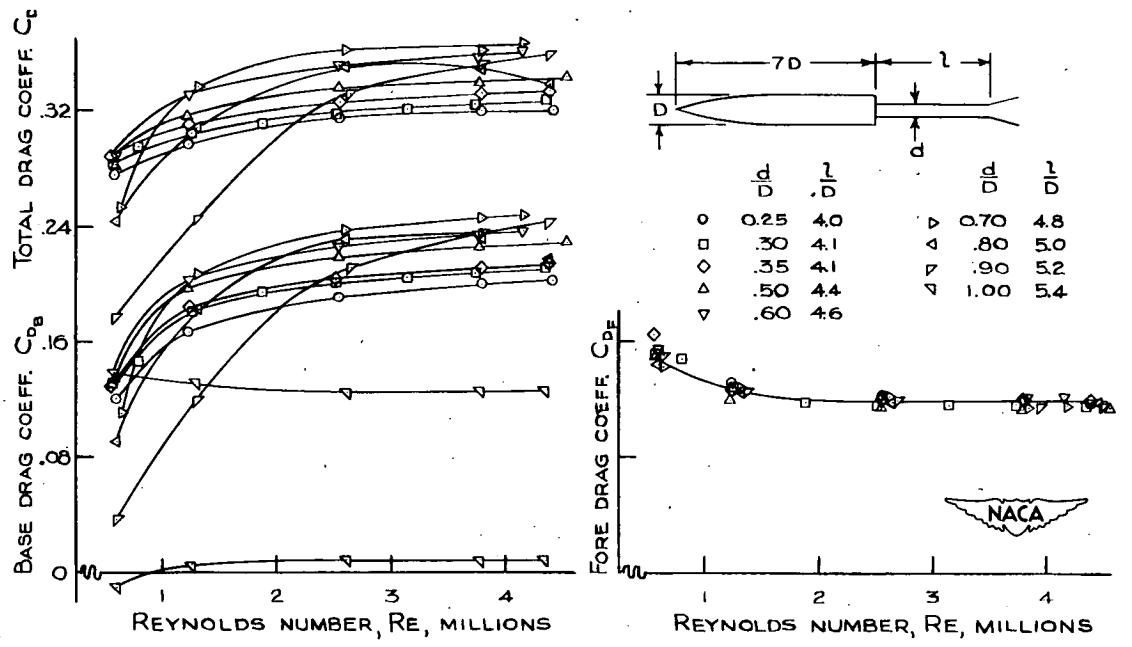

FIGURE 12.- VARIATION WITH REYNOLDS NUMBER OF THE DRAG CHARACTERISTICS OF MODEL 1 WITH SEVERAL REAR-SUPPORT DIAMETERS.

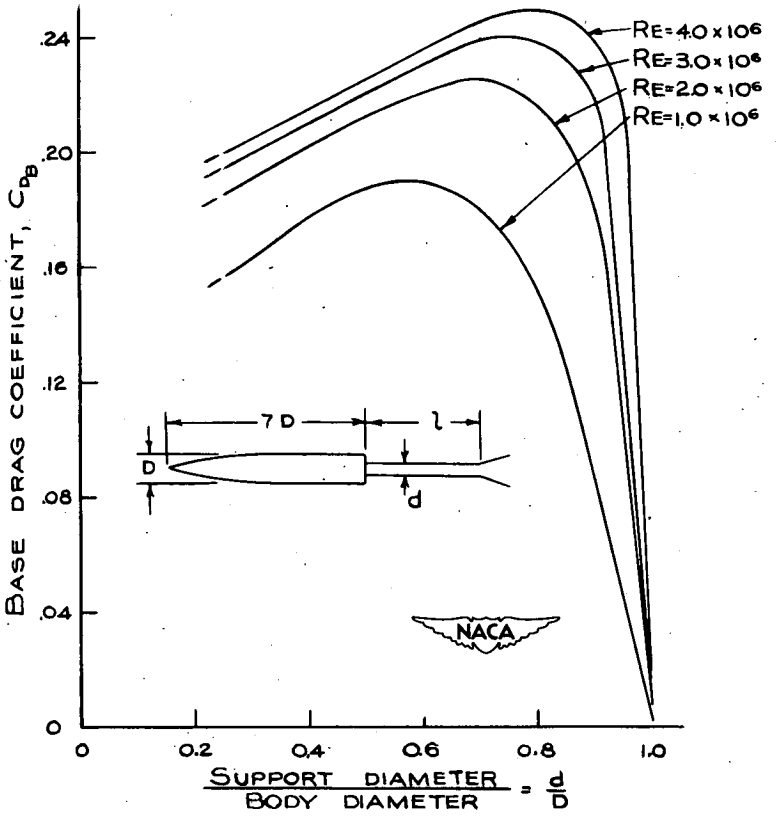

FIGURE 13.- VARIATION OF THE BASE DRAG COEFFICIENT WITH SUPPORT DIAMETER FOR MODEL 1.

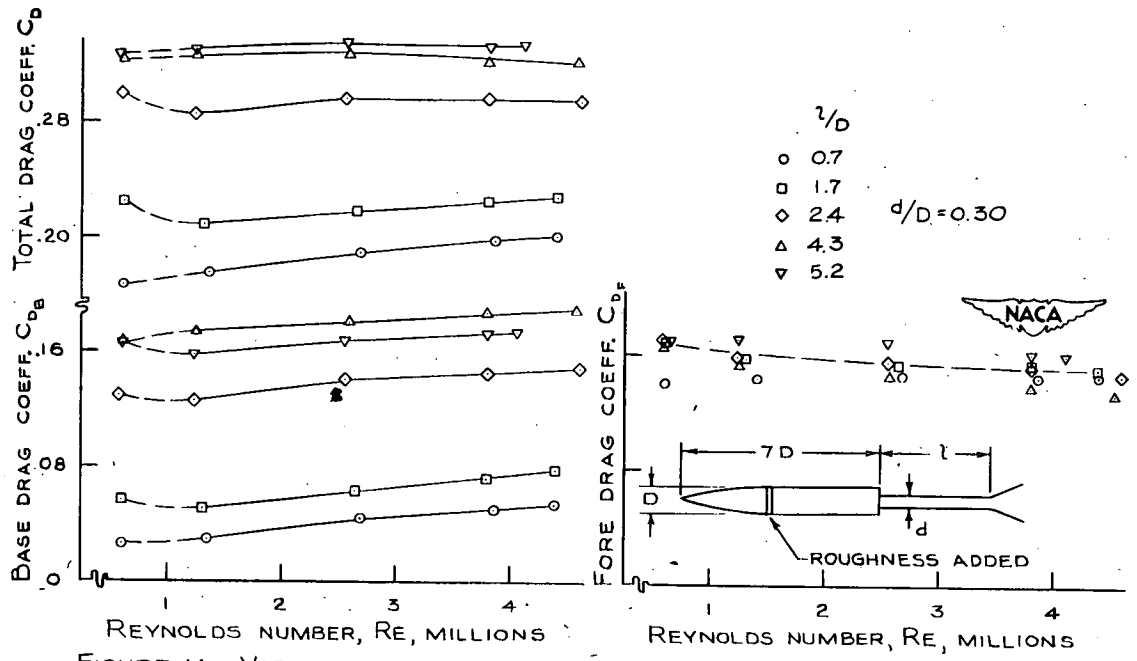

FIGURE 14.- VARIATION WITH REYNOLDS NUMBER OF THE DRAG CHARACTERISTICS OF MODEL 1 WITH ROUGHNESS ADDED FOR SEVERAL REAR-SUPPORT LENGTHS.

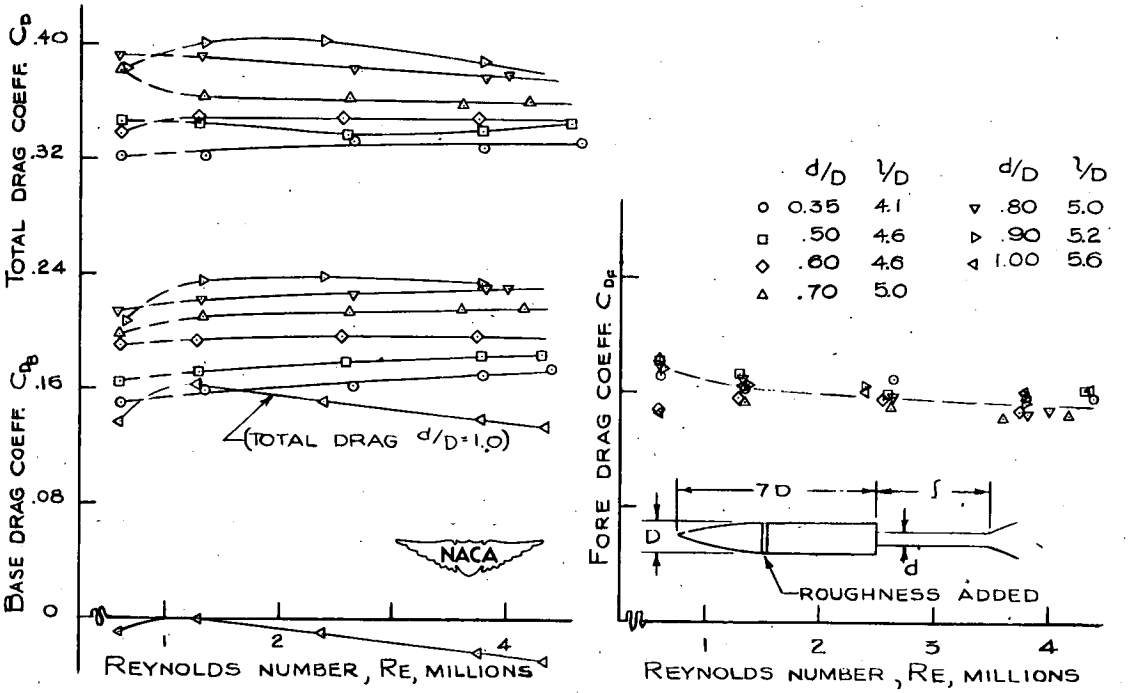

FIGURE 15.- VARIATION WITH REYNOLDS NUMBER OF THE DRAG CHARACTERISTICS OF MODEL 1 WITH ROUGHNESS ADDED FOR SEVERAL REAR-SUPPORT DIAMETERS.

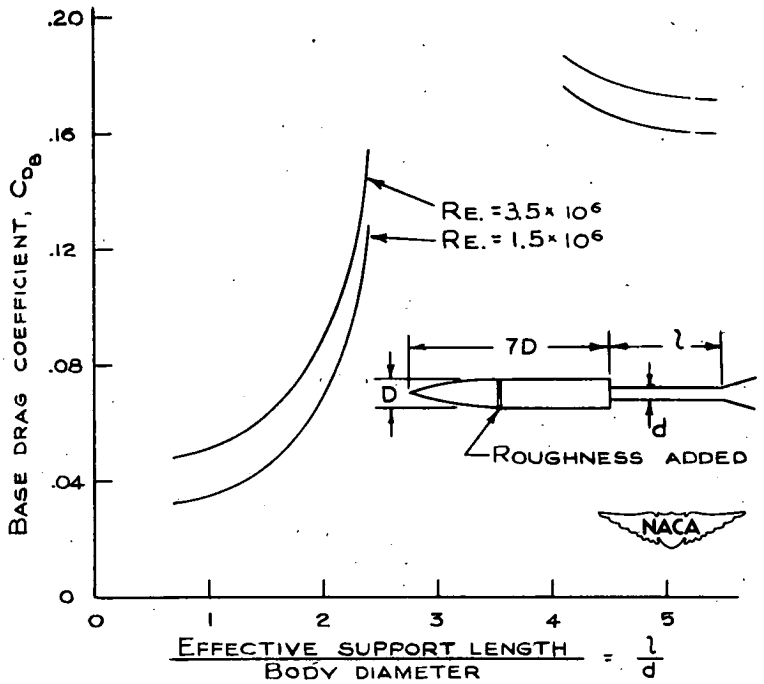

FIGURE 16.- VARIATION OF THE BASE DRAG COEFFICIENT WITH SUPPORT LENGTH FOR MODEL 1 WITH ROUGHNESS ADDED.

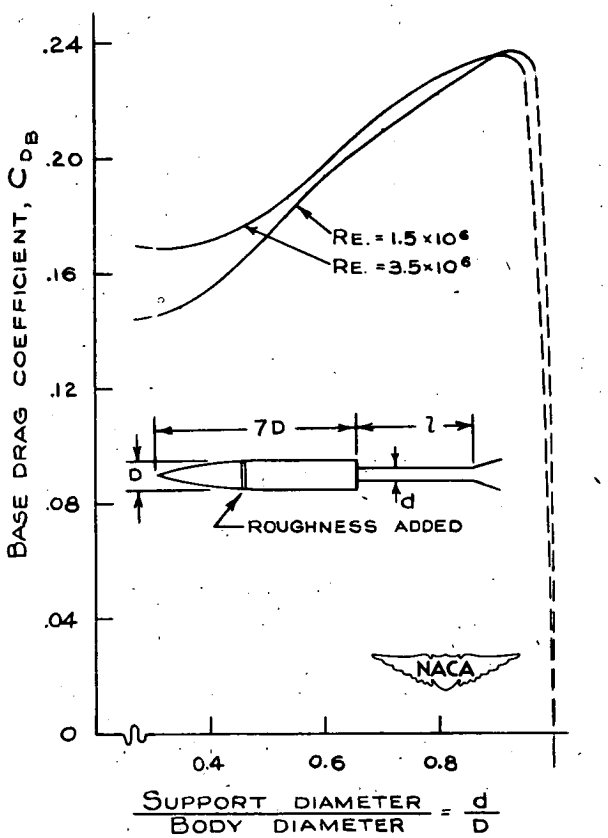

FIGURE 17.- VARIATION OF THE BASE DRAG COEFFICIENT WITH SUPPORT DIAMETER FOR MODEL 1 WITH ROUGHNESS ADDED.

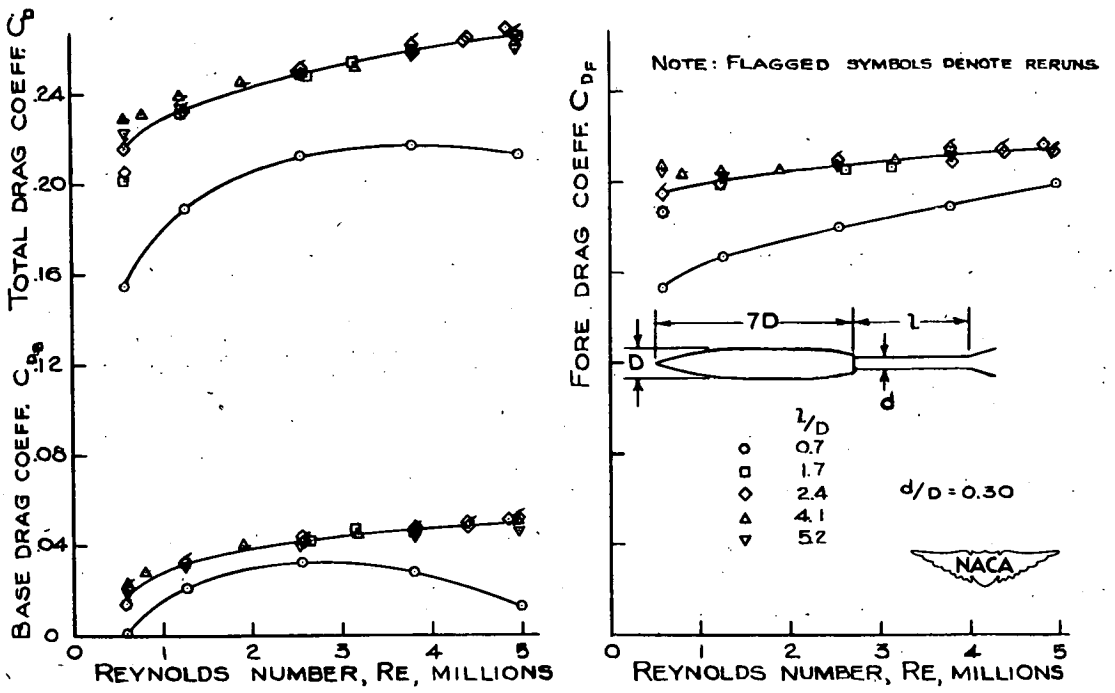

FIGURE 18.- VARIATION WITH REYNOLDS NUMBER OF THE DRAG CHARACTERISTICS OF MODEL 3 WITH SEVERAL REAR-SUPPORT LENGTHS.

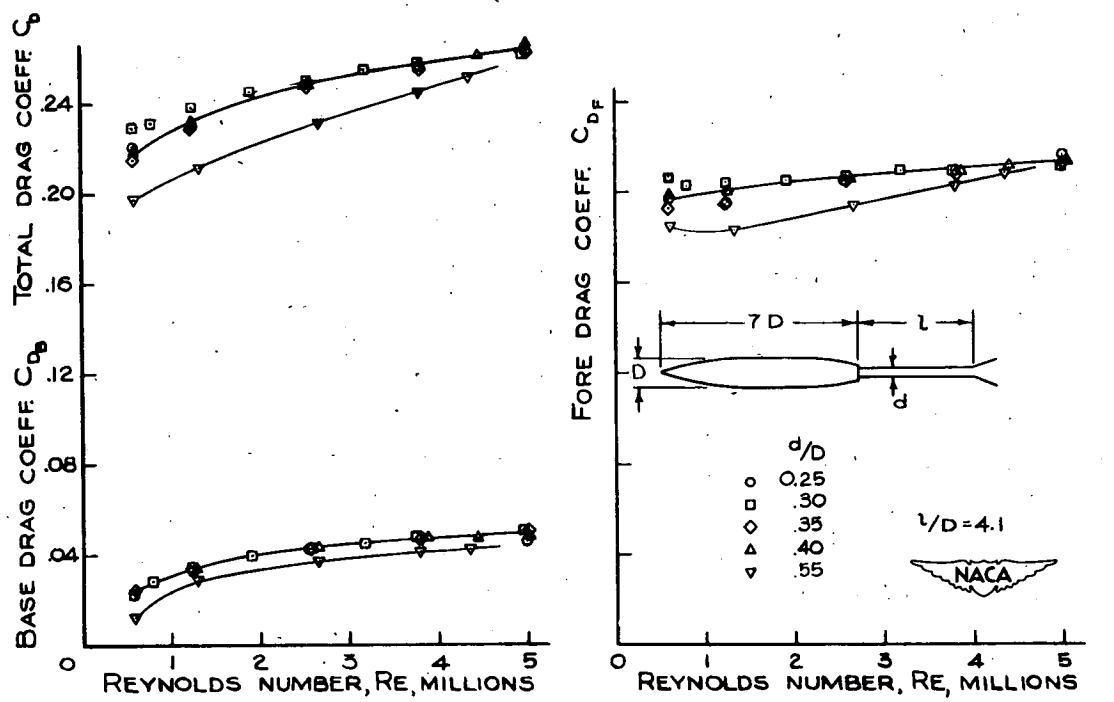

FIGURE 19.- VARIATION WITH REYNOLDS NUMBER OF THE DRAG CHARACTERISTICS OF MODEL 3 WITH SEVERAL REAR-SUPPORT DIAMETERS.

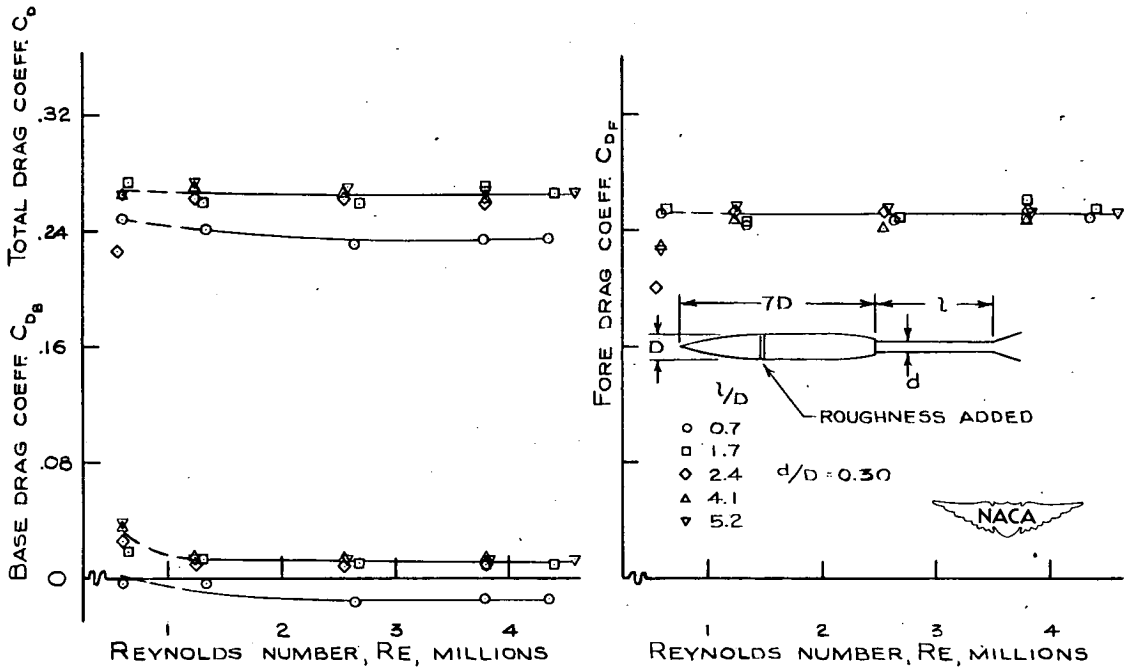

FIGURE 20.- VARIATION WITH REYNOLDS NUMBER OF THE DRAG CHARACTERISTICS OF MODEL 3 WITH ROUGHNESS ADDED FOR SEVERAL REAR-SUPPORT LENGTHS.

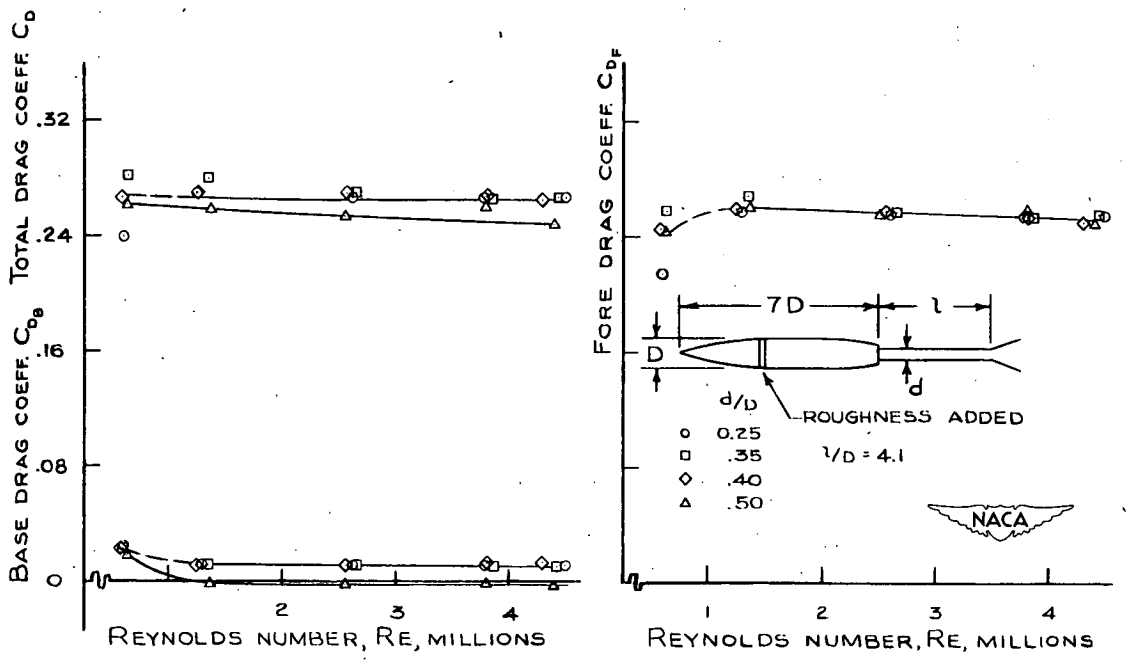

FIGURE 21.- VARIATION WITH REYNOLDS NUMBER OF THE DRAG CHACTERISTICS OF MODEL 3 WITH ROUGHNESS ADDED FOR SEVERAL REAR-SUPPORT DIAMETERS.

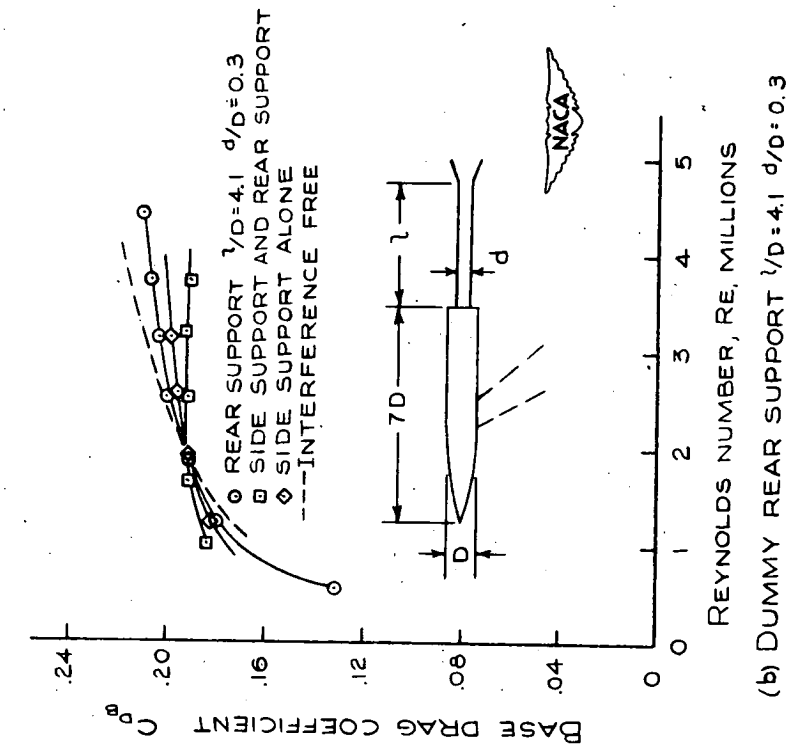

(b) Dummy rear support $l/D=4.1$ $d/D=0.3$

Figure 22.- Continued.

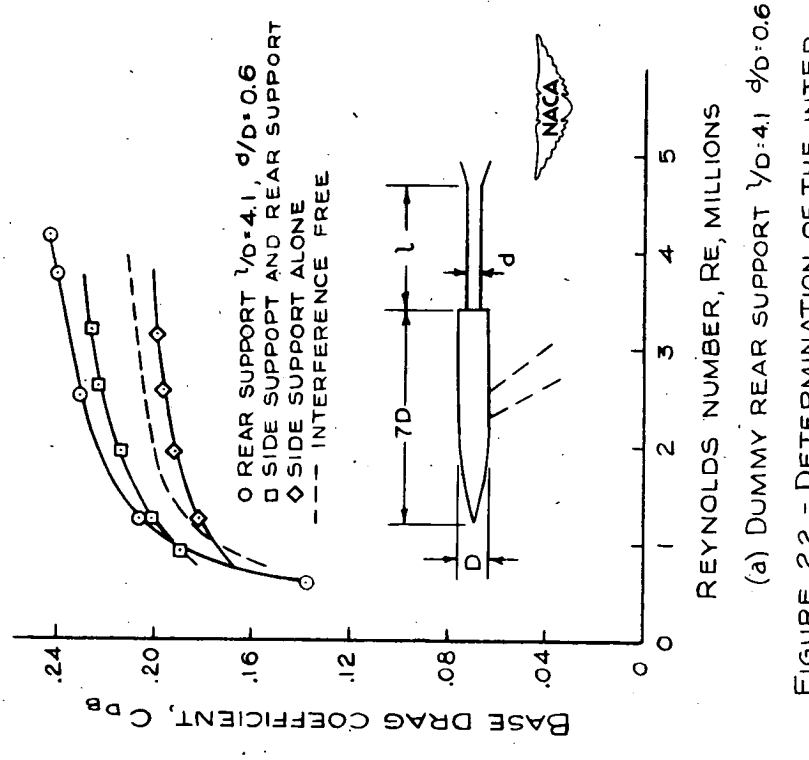

(a) Dummy rear support $l/D=4.1$ $d/D=0.6$

Figure 22.- Determination of the interference-free drag characteristics of model 1.

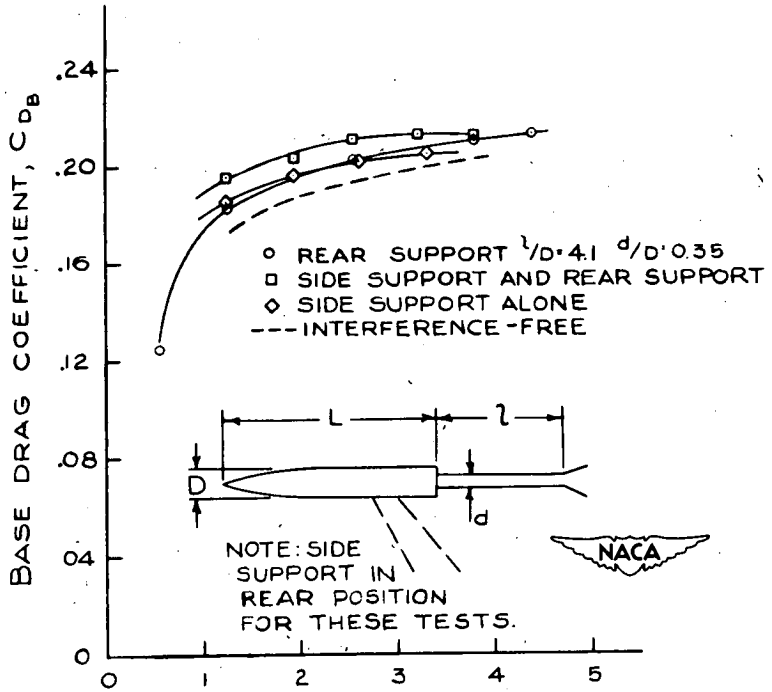

(c) DUMMY REAR SUPPORT l/D=4.1, d/D=0.35

FIGURE 22.- CONTINUED.

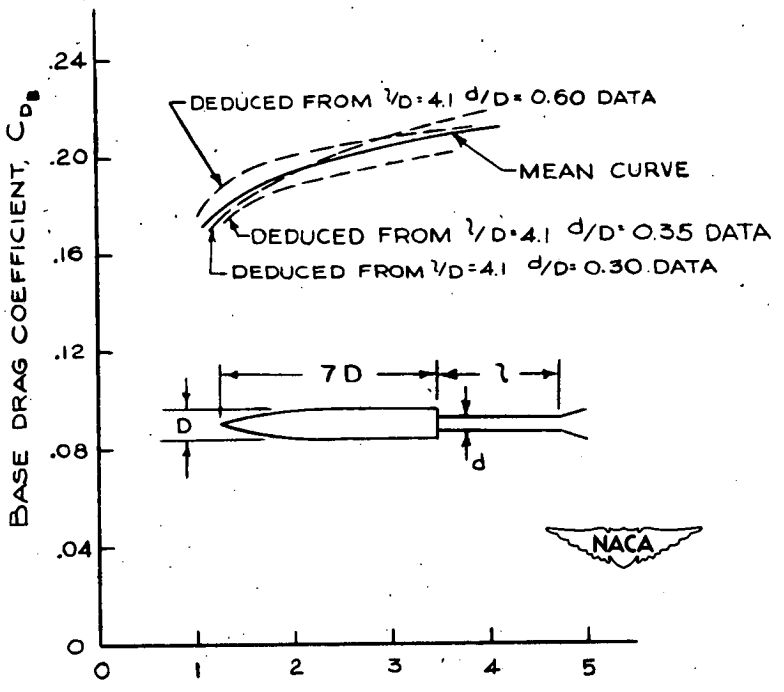

(d) MEAN INTERFERENCE-FREE CURVE.

FIGURE 22.- CONCLUDED.

NACA-Langley - 2-20-51 - 875